

Learning from straggler clients in federated learning

Andrew Hard^{**} Antonious M. Girgis^{†*} Ehsan Amid[‡]
 Sean Augenstein^{*} Lara McConnaughey^{*} Rajiv Mathews^{*} Rohan Anil[‡]
^{*}Google Research [†]University of California, Los Angeles [‡]Google DeepMind

Abstract

How well do existing federated learning algorithms learn from client devices that return model updates with a significant time delay? Is it even possible to learn effectively from clients that report back minutes, hours, or days after being scheduled? We answer these questions by developing Monte Carlo simulations of client latency that are guided by real-world applications. We study synchronous optimization algorithms like **FedAvg** and **FedAdam** as well as the asynchronous **FedBuff** algorithm, and observe that all these existing approaches struggle to learn from severely delayed clients. To improve upon this situation, we experiment with modifications, including distillation regularization and exponential moving averages of model weights. Finally, we introduce two new algorithms, **FARe-DUST** and **FeAST-on-MSG**, based on distillation and averaging, respectively. Experiments with the EMNIST, CIFAR-100, and StackOverflow benchmark federated learning tasks demonstrate that our new algorithms outperform existing ones in terms of accuracy for straggler clients, while also providing better trade-offs between training time and total accuracy.

1 Introduction

Cross-device federated learning (FL) [1] is a distributed computation paradigm in which a central server trains a global model by learning from data distributed across many client devices. Data heterogeneity and system heterogeneity across clients differentiate cross-device FL from other distributed optimization settings. Data heterogeneity refers to the fact that the data are not independently and identically distributed across clients (non-IID). System heterogeneity results from the many different device types that participate in training, each with different storage, communication, and computation constraints [2]. This heterogeneity leads to *straggler clients* in FL that take significantly more time to compute and return local model updates.

Standard FL algorithms such as **FedAvg** [1], **FedAdam** [3], and **FedProx** [4] utilize synchronous training rounds. In each round, a cohort of clients is sampled from a population. The clients receive a global model from the central server, update the model by processing locally cached training data, and upload the updated model back to the server. The server

^{*}Equal contribution

aggregates updated models from the clients in order to update the global model. In the synchronous setting, the server waits until all clients from the cohort (including stragglers) report back before updating the global model. The duration of each round is dictated by the slowest client in the cohort. Thus, synchronous FL algorithms can be slow to achieve a target accuracy in the presence of stragglers created by the natural heterogeneity of FL.

Production deployments perform cohort over-selection [5] to mitigate the impact of stragglers in FL. The orchestrating server selects a larger client cohort than required at the beginning of each FL round, uses the fastest clients to compute a global model update on the server, and discards the straggler client updates. Since the server doesn't have to wait for stragglers, over-selection significantly speeds up the training process and makes it robust to client dropouts. However, the final global model may be biased against stragglers.

Asynchronous optimization has been studied previously in server-based distributed settings [6, 7, 8, 9] as well as federated settings [10, 11, 12, 13]. Asynchronous FL abandons the notion of the synchronized round: the server schedules training on multiple clients in parallel and aggregates client updates as they are received. The decoupling of client computations and server updates speeds up training [11]. Convergence rates for asynchronous FL are proportional to the maximum client delay [14, 11, 15], though convergence is not always stable empirically.

Why do we care if global models are biased against straggler clients? In real-world FL, device characteristics (RAM, connection speed) may be correlated with socioeconomic factors. Failing to learn from straggler clients could result in models that perform poorly for certain groups within a population. In the hypothetical case of federated speech models, existing straggler mitigation techniques could result in higher word error rates for some dialects.

1.1 Summary of contributions

The goal of this work is to learn more effectively from straggler clients in FL, while maintaining competitive trade-offs for training time and overall accuracy. Our contributions are listed below.

- We construct a realistic Monte Carlo (MC) model for simulating client latency, based on observations of real-world applications of FL.
- We propose different client latency distributions in order to understand how FL algorithms utilize additional training examples and novel data domains from straggler clients.
- We measure the performance of existing algorithms such as **FedAvg**, **FedAdam**, and **FedBuff** in simulations with straggler clients, and identify improvements including exponential moving averages (EMA), knowledge distillation regularization, and proximal terms that improve the accuracy-training time trade-off.
- We propose two novel algorithms, **FARe-DUST** and **FeAST-on-MSG**, that are based on the concepts of knowledge distillation and EMA, respectively. These algorithms are capable of learning more from straggler clients with extreme time delays, while also training quickly and maintaining excellent overall accuracy.

1.2 Related work

Stragglers are a common problem for distributed learning. Prior works have explored mitigation based on data replication and coding theory [16, 17, 18]. These techniques are incompatible with FL because the central server (by design) cannot access client data [2]. Standard FL algorithms such as **FedAvg** [1] and its variants [3, 4, 19] utilize synchronous server updates that can be delayed by stragglers. **FedProx** [4] proposed assigning different local epochs for each client depending on their local computation speed. This approach does not account for communication latency, a significant source of delay. Cohort over-selection [5] can mitigate the delay caused by stragglers in synchronous FL, but it leads to under-representation of stragglers in the global model [12]. Finally, **InclusiveFL** [20] addresses the straggler under-representation issue by scaling the trainable model size according to the available client resources.

Xie et al. [10], Koloskova et al. [14], and Tsitsiklis et al. [21] studied a form of asynchronous stochastic gradient descent (async-SGD) in which the server updates the global model upon receipt of each client update. Methods have been proposed to down-weight straggler updates based on delay [22, 10, 23]. While such methods can improve total accuracy and training speed, they still induce a bias against straggler clients by down-scaling or dropping extremely delayed updates. **FedBuff** [11, 12] eschews down-weighting and aggregates client updates in a buffer before updating the global model.

Probabilistic wall clock training time models have been explored previously for distributed ML [24] and FL [25, 26, 13]. Prior works mostly focus on a shifted-exponential parameterization of latency and assume that runtime is proportional to the number of steps of SGD. All computation nodes feature the same latency distribution, and stragglers are distinguished only by having more training points.

Global model performance for straggler clients has also been explored in multiple contexts. Huba et al. [12] showed that **FedAvg** with over-selection biased the training distribution and led to worse performance for clients with many examples, while **FedBuff** did not. Charles et al. [26] explored fairness via the impact of cohort size on accuracy for individual client datasets.

Scenarios in which key data domains exist predominantly on straggler clients have not been explored thoroughly. Such cases are important for real-world FL, since stragglers often correspond to older and cheaper devices and may be correlated with socioeconomic factors. Excluding stragglers may create models that are biased and not representative of the entire population. Our work explores problems in which straggler clients feature unique data domains that are not present on fast clients.

2 Algorithms

Let $f(w, x)$ denote the loss of model w on example x . We considered the FL framework for solving the optimization problem: $\min_{w \in \mathbb{R}^d} \frac{1}{m} \sum F_i(w)$, where m is the total number of clients and $F_i(w) = \mathbb{E}_{x \sim \mathcal{D}_i} [f(w, x)]$ is the loss function of the i th client, with local dataset \mathcal{D}_i .

We studied the performance of multiple FL algorithms for straggler clients. A few canonical baseline algorithms were considered, as well as modified versions of these baselines

that were intended to learn more from stragglers. Finally, we developed two entirely new algorithms, **FARe-DUST** and **FeAST-on-MSG**, that were designed to learn from straggler clients with arbitrary delays.

2.1 Baseline federated algorithms and modifications

FedAvg [1] and **FedAdam** [3] were used as synchronous FL baselines. Both algorithms were trained with and without cohort over-selection. **FedBuff** [11] was chosen as an asynchronous FL baseline.

Since the baseline algorithms were originally designed to maximize performance across an entire client population, we tested various modifications that would enable them to learn more from straggler clients. For the synchronous algorithms, we experimented with *time-limited client computations*. In this technique, clients computed as many local steps of SGD as they could before reaching a maximum training time limit (not step limit). We chose to set time limits to the population-wide 75th percentile on-device computation times for one local training epoch. The time limit did not apply to the communication latency. While this modification still led to more training steps on fast client data, it ensured that straggler clients could report back at least partial training results quickly.

FedBuff was unstable in preliminary experiments with extremely delayed clients, so we tested multiple techniques to smooth the convergence. The first was *distillation regularization* [27, 28], in which the most recent global model weights were sent to each client and used as a teacher network for distillation during local training. The teacher loss was interpolated with the supervised loss function using a small regularization factor. The second **FedBuff** addition we explored was adding a *proximal term* to the client loss function [4]. This regularization helped reduce client drift [29] for stragglers. Third, we tested *exponential moving averages* (EMA) of model weights [30]. EMA models have been shown to generalize better than weights from individual time steps. For asynchronous algorithms, EMA might smooth out vast differences between time steps. Finally, we experimented with applying Adam instead of SGD to the **FedBuff** server update step, since adaptive optimizers significantly improve synchronous FL [3].

2.2 FARE-DUST algorithm

Our first algorithm, **FARe-DUST** (Federated Asynchronous Regularization with Distillation Using Stale Teachers), incorporates stale updates from straggler FL clients into a global model using co-distillation [28]. The key insight from prior co-distillation works is that students can benefit from stale, partially trained teacher networks.

Our algorithm builds upon **FedAvg**. At each round $t \in T$, the server samples a set \mathcal{C}_t of size $B_t = |\mathcal{C}_t|$ clients uniformly at random from the population. The global model is updated as soon as the server receives the $B < B_t$ local updates from the fastest subset of clients, $\mathcal{C}_t^{\text{fast}}$. The fast client weight deltas (Δ_t^c for $c \in \mathcal{C}_t^{\text{fast}}$) are summed to produce Δ_t , which is applied as a pseudo-gradient to the global model¹: $w_{t+1} = w_t - \frac{\eta g}{B} \Delta_t$. So far, this is equivalent to **FedAvg**.

¹We show the SGD update for simplicity, though other server optimizers (e.g., Adagrad, Adam, and Yogi) may be utilized in FL.

FARe-DUST diverges from FedAvg by storing the past k summed *historical* model deltas (Deltas = $\{\Delta_{t-k}, \dots, \Delta_t\}$). When straggler clients from round t' (for $t - k \leq t' < t$) belatedly report back to the server, their updates are summed into a corresponding historical model delta $\Delta_{t'}$. Thus, $\Delta_{t'}$ includes updates from stragglers as well as fast clients. These weight deltas are subsequently used to create *teachers* for distillation on clients.

Teacher networks are constructed by uniformly randomly sampling a historical model delta Δ_{teacher} from Deltas and applying it to the *latest* model weights: $w_{\text{teacher}} = w_t - (\eta_g/B_{\text{teacher}})\Delta_{\text{teacher}}$. Stragglers thus contribute to the historical model deltas, which create the teacher networks that distill straggler knowledge into subsequent cohorts of clients. As computation input, each sampled client receives the most recent global model, w_t , as well as one teacher network, w_{teacher} . A different teacher is sampled for every client in every round.

Clients in FARE-DUST run multiple iterations of SGD to update the local model. For a given client i , the client loss at iteration t is the sum of two functions: the local loss function $F_i(w_t^i)$ from training on the local client data, and the distillation loss $\psi_i(w_t^i, w_{\text{teacher}})$ for the historical teacher model w_{teacher} logits and student outputs on the local dataset \mathcal{D}_i . Local update step t for client i is therefore given by

$$w_{t+1}^i = w_t^i - \eta_l \nabla_{w_t^i} (F_i(w_t^i) + \rho \psi_i(w_t^i, w_{\text{teacher}})),$$

where $\rho \geq 0$ governs the distillation regularization strength. Since the teacher model w_{teacher} has updates from stragglers, the new global model can learn from the stale updates of the stragglers.

See Algorithm 1 in Appendix A for the complete FARE-DUST procedure. At the end of training, the EMA of the global model weights is used for inference.

2.3 FeAST-on-MSG algorithm

Our second FL algorithm is FeAST-on-MSG (Federated Asynchronous Straggler Training on Mismatched and Stale Gradients). The core idea is to transfer information from early round stragglers to later rounds via an *auxiliary model*. FeAST-on-MSG builds on EMA [30], and the fact that weight averaging over many steps (including stale steps) improves performance.

Let τ_{max} denote the maximum amount of time that we allow the straggler clients to report back their local updates at each round. At the server, we maintain the global model weights w_t along with *auxiliary model weights* a_t at round t . As in FedAvg and FARE-DUST, we update the global weights to get w_{t+1} using updates from the $B \leq B_t$ fastest clients $\mathcal{C}_t^{\text{fast}}$ that report back to the server. The global weights w_{t+1} are used to start the next round of FL. However, we keep track of the global model weights w_t and gradient Δ_t for the duration of τ_{max} . In the meantime, we accumulate any additional gradient from stragglers at round t within the τ_{max} time interval. Within τ_{max} , we combine the model differences from the straggler clients $\mathcal{C}_t^{\text{slow}} \subseteq \mathcal{C}_t \setminus \mathcal{C}_t^{\text{fast}}$ at round t that successfully report back with the model difference from the fast clients Δ_t to form

$$\Delta_t^+ = \Delta_t + \sum_{c \in \mathcal{C}_t^{\text{slow}}} \Delta_t^c. \quad (1)$$

We use Δ_t^+ to form w_{t+1}^+ , based on w_t : $w_{t+1}^+ = w_t - (\eta_g/B_t^+)\Delta_t^+$, where η_g is the global model learning rate and $B_t^+ = |\mathcal{C}_t^{\text{fast}}| + |\mathcal{C}_t^{\text{slow}}|$.

In general, we expect w_{t+1}^+ to correspond to a slightly improved version of w_{t+1} , as we use a larger client cohort for the update step. However, we cannot replace the global model weights for the next round w_{t+1}^+ , as the client updates at round $t + 1$ are already calculated using w_{t+1} . While the error due to the mismatched weights and client updates may not be large for a single round, the accumulated error over multiple rounds can significantly deteriorate the performance. Therefore, we utilize the auxiliary model weights a_t as a form of *weight averaging* to reduce the effect of mismatched weights. Specifically, we write the auxiliary model weights update as

$$a_{t+1} = \beta(a_t - \frac{\eta_a}{B_t^+} \Delta_t^+) + (1 - \beta)w_{t+1}^+, \quad (2)$$

where $\eta_a > 0$ is the auxiliary model learning rate and $\beta \in (0, 1)$ denotes the EMA decay. The auxiliary model update in Equation (2) has interesting interpretations based on the value of η_a . For $\eta_a = 0$ (and assuming $a_0 = w_0^+ = w_0$), the auxiliary model update reduces to an EMA of the past models, with a decay factor of β : $a_{t+1} = \beta a_t + (1 - \beta)w_{t+1}^+$. Alternatively, when $\eta_a = \eta_g$, the updated auxiliary model is formed via a gradient step on a weighted average of the current auxiliary and global models using the aggregated model differences Δ_t^+ : $a_{t+1} = (\beta a_t + (1 - \beta) w_t) - \frac{\eta_g}{B_t^+} \Delta_t^+$. Algorithm 2 in Appendix A provides a complete description of FeAST-on-MSG.

3 Client latency modeling

This section describes our MC models of client latency. Realistic client latency simulations are essential for measuring how well FL algorithms learn from stragglers. Observations from production FL systems are provided in Appendix C.

3.1 Components of client latency

Wang et al. [31] provided a framework for modeling FL round and client execution time. The total run time is a sum of server-client communication time and client computation time: $T_{\text{round}} = T_{\text{communication}} + T_{\text{computation}}$, where $T_{\text{computation}} = C + (T_{\text{per-example}} \cdot N_{\text{examples}})$. C is a system overhead constant for clients, and includes the start-up and turn-down time associated with the client computations. It does not scale with the number of training examples. $T_{\text{per-example}}$ is the time required to process each local training step on clients, and $T_{\text{communication}}$ is the communication time, including both the client download time and the server upload time.

3.2 Monte Carlo latency simulation

We directly modeled distributions of C , $T_{\text{per-example}}$, and $T_{\text{communication}}$ with log-normal functions. Download and upload latency were not modeled separately, since the two are strongly correlated in practice. N_{examples} corresponded to the simulated client dataset size $|\mathcal{D}_i|$.

Client latencies were randomly generated via Monte Carlo techniques during FL simulations. Each client was assigned a particular μ and σ for each latency parameter at the

Table 1: Latency factor parameterizations for all clients in the `per-example` client latency model.

Latency factor	Parameterization
$T_{\text{communication}}$	Lognormal($\mu = 2.7, \sigma = 1.0$)
$T_{\text{per-example}}$	Lognormal($\mu = -1.6, \sigma = 0.5$)
C	Lognormal($\mu = 3.0, \sigma = 0.3$)

beginning of training. During each FL round, clients in the cohort randomly sampled latency values from their parameter distributions. Thus, clients sampled different latency values each time they participated in training.

3.3 Latency models

In order to better understand how straggler clients affect the training time and performance of various FL algorithms, we explored two client latency models: `per-example` and `per-domain per-example` client latency. In particular, we were interested in whether algorithms that learned more from stragglers benefited more from additional data volume, additional data domains, or both.

The `per-example` client latency model is a stochastic model in which client computation times scale with the number of examples in the local client data. Latency factors were sampled from the MC model described in Section 3.2 for each client during each round of FL. Specific parameterizations of the latency factors are summarized in Table 1. This setting was useful for exploring the impact of the additional data available on straggler clients, since stragglers were only distinguished by the amount of local data and not data domain.

The `per-domain per-example` client latency model is a stochastic model in which clients with examples from specific data domains are assigned significantly higher latencies. This model builds on the `per-example` model by scaling client computation times with the number of client examples. However, certain clients (pre-selected according to data domain) were assigned distributions of $T_{\text{communication}}$, $T_{\text{per-example}}$, and C with higher median times and longer tails. Parameterizations of the latency factors for standard clients and straggler clients are summarized in Table 2. The differences between the data domains of standard clients and straggler clients in this setting enabled us to explore how FL algorithms learned from novel data domains found only on straggler clients.

4 Datasets and tasks

4.1 Federated tasks

Experiments were conducted with three popular FL benchmark tasks: two dense gradient tasks (EMNIST [32] and CIFAR-100 [33] classification), and one sparse gradient task (StackOverflow [34] next-word prediction).

Table 2: Latency factor parameterizations for the **per-domain per-example** client latency model. Larger μ values were used for the straggler clients, resulting in higher medians and longer tails.

Latency factor	Parameterization	
	Standard clients	Straggler clients
$T_{\text{communication}}$	Lognormal($\mu = 2.7, \sigma = 1.0$)	Lognormal($\mu = 3.7, \sigma = 1.0$)
$T_{\text{per-example}}$	Lognormal($\mu = -2.0, \sigma = 0.2$)	Lognormal($\mu = -1.0, \sigma = 0.5$)
C	Lognormal($\mu = 3.0, \sigma = 0.3$)	Lognormal($\mu = 3.5, \sigma = 0.3$)

The EMNIST training data consists of handwritten characters converted into a 28×28 pixel image format. To create a simulated non-IID FL dataset, EMNIST examples were partitioned into client clusters based on the writer. We then selected a subset of EMNIST clients to represent stragglers. First, we defined the digits 0-4 as **straggler classes**. Next, we found the 800 clients with the most examples from those straggler classes and defined them as the **straggler clients**. Finally, all examples from the straggler classes were removed from non-straggler clients, which were referred to as **standard clients**. Thus, training examples from straggler classes resided exclusively in the 800 straggler client data partitions. Overall, there were 3,400 simulated FL clients for EMNIST (2,600 standard and 800 straggler clients).

The CIFAR-100 data contains 50,000 RGB images of size $32 \times 32 \times 3$ from 100 classes. We used the non-IID partitioning of the CIFAR-100 dataset proposed in [3], which created 500 clients with 100 examples each, using a two-step LDA process over the coarse and fine labels. Similar to the procedure for generating straggler clients for EMNIST, we first defined the “vehicles 1” and “vehicles 2” coarse classes as the straggler classes. As with EMNIST, we selected the 125 clients with the most straggler class examples as the straggler clients. Any examples from the straggler classes were then removed from the 375 remaining standard clients.

StackOverflow training data consists of textual question-and-answer posts to the eponymous website along with associated subject tags. Data were partitioned into simulated FL clients based on user ID. Examples with the “math” and “c + +” tags were chosen as the straggler classes for StackOverflow. All clients with at least one training example with one of these tags were labeled as straggler clients. This procedure resulted in a dataset consisting of 342,477 clients (248,595 standard and 93,882 straggler clients). Questions and answers with the straggler classes (“math” and “c + +” tags) were found exclusively on the straggler clients.

We used the same model architectures as in Reddi et al. [3] for each task: a CNN model [35, 36, 37] for EMNIST, a ResNet-18 model [38] for CIFAR-100, and an LSTM [39] for StackOverflow.

4.2 Data and latency models

The **per-example** and **per-domain per-example** client latency models described in Section 3.3 were explored in conjunction with the 3 FL tasks. Latency statistics sampled from

Table 3: Simulated client latencies with the EMNIST dataset, using the **per-example** latency model (left) and **per-domain per-example** latency model (right).

	per-example			per-domain per-example		
	50% [s]	95% [s]	99% [s]	50% [s]	95% [s]	99% [s]
Standard clients	69.89	151.7	223.4	59.35	117.3	194.3
Straggler clients	77.14	160.5	223.8	151.5	323.8	472.0

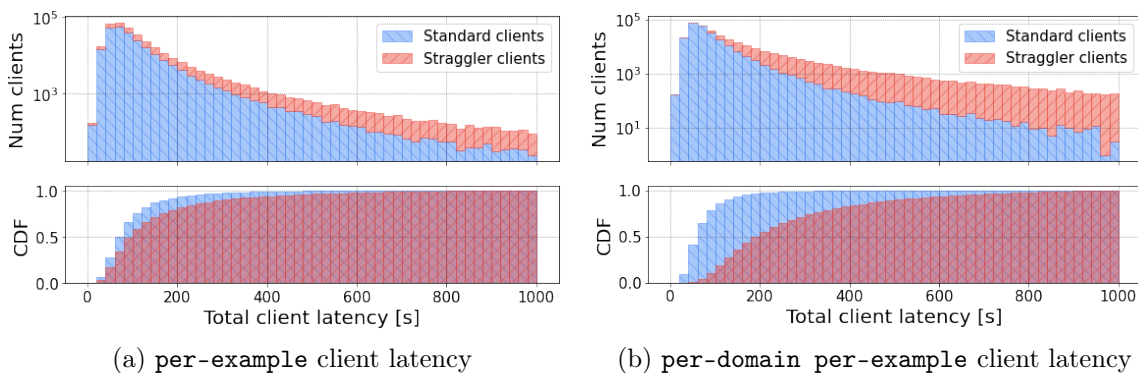


Figure 1: The distribution of total client latencies, in seconds, sampled for the StackOverflow dataset with the **per-example** (Figure 1a) and **per-domain per-example** client latency models (Figure 1b). PDFs (top) are stacked, while the CDFs (bottom) are overlaid.

one epoch over the EMNIST dataset are shown in Table 3 for both the **per-example** and **per-domain per-example** client latency models. With the **per-example** scenario, straggler and standard client latencies were quite similar across percentiles. For the **per-domain per-example** model, however, straggler clients were $3\times$ slower than standard clients across all percentiles. The median straggler was slower than the 99th percentile standard client.

Appendix F provides distributions and statistics for each dataset and latency model combination. For the CIFAR-100 task with the **per-example** latency model, the straggler and standard clients had comparable latency distributions. With the **per-domain per-example** model, CIFAR-100 straggler clients were $3\times$ slower than standard clients at the 99th percentile.

Figure 1 shows a histogram of the client latencies for StackOverflow. With the **per-example** latency model, standard and straggler clients had comparable median latencies (80.64s vs. 106.1s, respectively). Straggler clients (with “math” and “c + +” tags) had more examples than average. For the **per-domain per-example** latency model, the 99th percentile straggler was $10\times$ slower than the 99th percentile standard client.

5 Experiments

FedAvg, FedAdam, FedBuff, FeAST-on-MSG, and FARE-DUST were compared on the six combinations of task and latency models described in Section 4.2. FL simulations were conducted

using the FedJAX framework [40]. Training hardware consisted of a 2×2 configuration of V3 TPUs [41].

5.1 Metrics

We defined a **straggler accuracy** metric that measured model accuracy on held-out examples belonging to the straggler data classes defined in Section 4.1. This metric corresponded to classification accuracy on digits 0-4 for EMNIST and “vehicles 1” or “vehicles 2” for CIFAR-100. With StackOverflow, straggler accuracy was defined as next-word prediction accuracy for in-vocabulary tokens on posts with the “math” or “c + +” tags. The only way to improve straggler accuracy was by learning effectively from straggler clients.

We also measured total classification accuracy for EMNIST and CIFAR-100, and total in-vocabulary next-word prediction accuracy for StackOverflow. This enabled us to observe whether standard client accuracy regressed when straggler accuracy improved. The number of aggregated client updates, training steps, and total wall-clock training time were also tracked for each experiment.

5.2 Tuning

The objective of tuning was to maximize straggler accuracy. Total accuracy, total training time, and consistency across trials were not *explicitly* optimized during the tuning process. Algorithms were tuned separately for all datasets and latency models. Default hyperparameter values for **FedAvg** and **FedAdam** were adopted from [3]. Learning rates, buffer size, and concurrency were tuned for **FedBuff**, while 3 parameters were tuned for both **FARe-DUST** and **FeAST-on-MSG**. Tuning procedures and optimal hyperparameter values are provided in Appendix G.

Training was performed for a fixed number of client updates, in order to provide fair comparisons between synchronous and asynchronous algorithms. EMNIST tasks were trained using 100,000 client updates (equivalent to 2,000 rounds of **FedAvg** with a cohort of 50 clients), CIFAR-100 tasks were trained using 80,000 client updates (4,000 rounds of **FedAvg** with a cohort of 20), and StackOverflow tasks were trained using 200,000 client updates (2,000 rounds of **FedAvg** with a cohort of 100).

6 Results

Figure 2 shows straggler accuracy and total accuracy as a function of wall-clock training time, for the EMNIST task and **per-domain per-example** client latency model. **FeAST-on-MSG** and **FARe-DUST** both converged the fastest to the highest straggler accuracy, and **FARe-DUST** also achieved the highest total accuracy. Interestingly, **FeAST-on-MSG** was over-tuned for straggler accuracy and had low total accuracy. **FedBuff** trained quickly, but had poor straggler accuracy and very high-variance performance. **FedAdam** and **FedAvg** were consistent, but slow to converge and failed to reach high straggler accuracy.

CIFAR-100 results with the **per-domain per-example** client latency model are shown in Figure 3. **FARe-DUST** and **FeAST-on-MSG** achieve the 1st and 3rd highest straggler accuracy

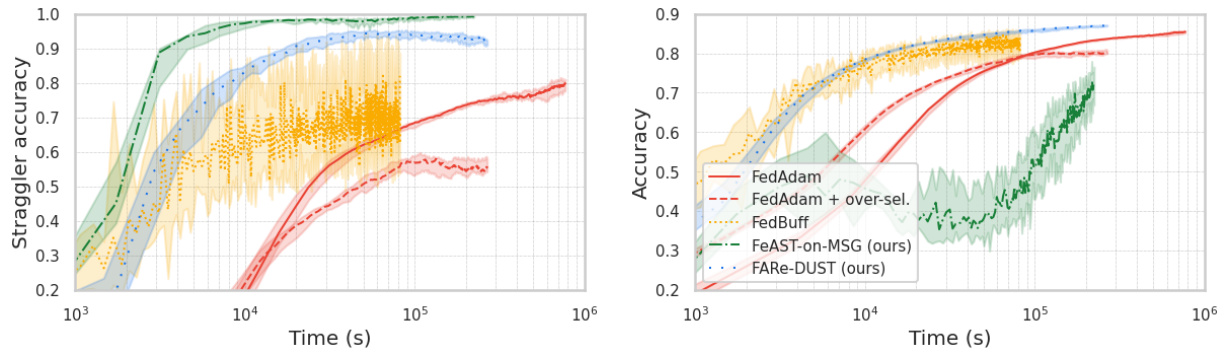


Figure 2: Straggler accuracy (left) and total accuracy (right) as a function of wall clock training time for EMNIST with the **per-domain per-example** latency model. Solid lines and bands represent the median and 90% confidence intervals from 10 trials.

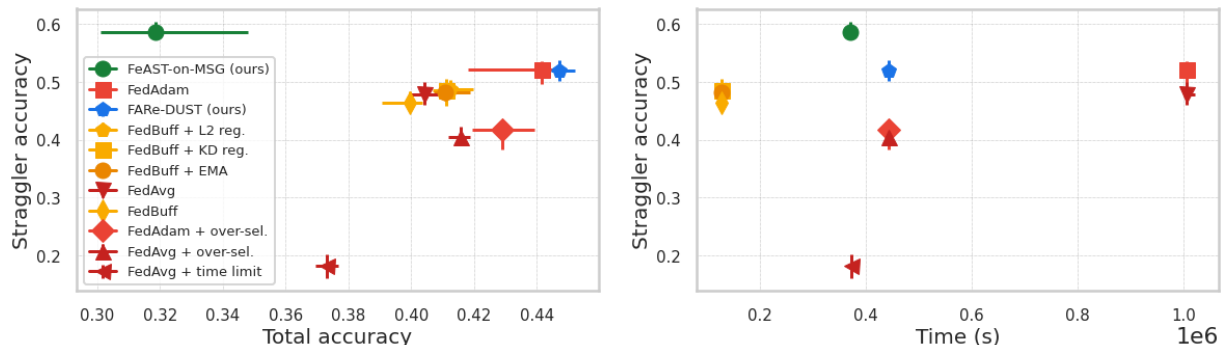


Figure 3: Straggler accuracy as a function of total accuracy (left) and wall clock training time (right) for CIFAR-100 with **per-domain per-example** latency model. Plots show the median and 90% CI from 10 trials for the best straggler accuracy value in each trial.

values, while training more than $2.5\times$ faster than **FedAdam** which had the 2nd highest straggler accuracy. While **FedBuff** converges quickly, it fails to reach competitive total or straggler accuracy values.

Results with the **per-example** client latency model and StackOverflow task are summarized in Table 4. Values are provided for **FedAvg** and **FedAdam** with and without over-selection and with time-limited client computations. Comparisons are shown for **FedBuff** with EMA and knowledge distillation regularization. While **FedAdam** achieved the highest straggler accuracy, it was more than $10\times$ slower than **FeAST-on-MSG** and **FARe-DUST**, which ranked second. **FedBuff** once again had low straggler accuracy and total accuracy, though EMA and KD were beneficial. Interestingly, over-selection did not hurt synchronous algorithms on this task.

Appendix B discusses all of the findings above in detail, and Appendix H provides comprehensive numerical results for every task, latency model, and algorithm. The primary empirical observations are summarized below.

- **FARe-DUST** was the most consistently high-performing algorithm in terms of straggler

Table 4: The straggler accuracy, total accuracy, and the total training time for each algorithm with the StackOverflow dataset and `per-example` client latency model. Median and 90% CI values from 10 trials are quoted for each metric. Rows are sorted in descending order of straggler accuracy.

Algorithm	Straggler accuracy		Total accuracy		Time [s]
	Median	95% CI	Median	95% CI	
FedAdam	25.6%	[25.5%, 25.7%]	25.4%	[25.1%, 25.9%]	3,612,004
FeAST-on-MSG	25.2%	[24.6%, 25.3%]	26.1%	[25.2%, 26.7%]	292,006
FARe-DUST	25.0%	[24.5%, 25.2%]	25.4%	[24.3%, 26.4%]	335,744
FedAdam + over-sel.	24.9%	[23.3%, 25.0%]	25.2%	[21.8%, 25.9%]	336,140
FedBuff + EMA	24.3%	[24.2%, 24.3%]	24.6%	[23.3%, 26.0%]	349,178
FedBuff + KD reg.	24.2%	[24.2%, 24.3%]	23.9%	[23.4%, 25.1%]	350,286
FedAvg	23.7%	[23.5%, 23.8%]	23.6%	[22.2%, 24.6%]	3,584,260
FedBuff	23.3%	[22.3%, 23.6%]	23.4%	[22.3%, 23.7%]	349,257
FedAvg + time limit	21.7%	[21.7%, 21.7%]	22.7%	[21.3%, 23.4%]	287,952
FedAvg + over-sel.	20.9%	[20.8%, 20.9%]	22.4%	[21.1%, 23.2%]	407,588

accuracy, across tasks and latency models.

- **FeAST-on-MSG** provided the highest straggler accuracy on most tasks and a good trade-off between total accuracy and time. It had a tendency to over-tune on straggler accuracy.
- **FedBuff** converged faster but to lower accuracy than other algorithms on most tasks. Modifications such as EMA, distillation regularization, and adaptive optimizers improved the straggler accuracy and total accuracy for **FedBuff**.
- Over-selection sped up synchronous algorithms and even boosted accuracy in the `per-example` latency scenario. However, it generally led to worse total accuracy and straggler accuracy in the `per-domain per-example` latency scenario.
- Limiting client computations by time sped up training for **FedAvg** at the cost of reduced straggler accuracy for the `per-domain per-example` latency scenario. Stragglers only trained for a fraction of a local epoch, while standard clients processed more than 1 epoch.

7 Conclusion

This work explored methods for learning from straggler clients with extreme delays in FL. Through simulation experiments with MC latency models on EMNIST, CIFAR-100, and StackOverflow, we found that our proposed algorithms — **FARe-DUST** and **FeAST-on-MSG** — significantly improved the accuracy of global models for straggler clients. Furthermore, these algorithms provided trade-offs of total accuracy and training time that were better than those

offered by existing algorithms. Finally, we identified techniques such as EMA and distillation regularization that improved baselines like FedBuff. Given the growth of cross-device FL applications in which device heterogeneity mirrors socioeconomic status, it is imperative that FL models are reflective of the whole population.

References

- [1] Brendan McMahan, Eider Moore, Daniel Ramage, Seth Hampson, and Blaise Agueray Arcas. Communication-efficient learning of deep networks from decentralized data. In *Artificial intelligence and statistics*, pages 1273–1282. PMLR, 2017.
- [2] Peter Kairouz, H Brendan McMahan, Brendan Avent, Aurélien Bellet, Mehdi Bennis, Arjun Nitin Bhagoji, Kallista Bonawitz, Zachary Charles, Graham Cormode, Rachel Cummings, et al. Advances and open problems in federated learning. *Foundations and Trends® in Machine Learning*, 14(1–2):1–210, 2021.
- [3] Sashank Reddi, Zachary Charles, Manzil Zaheer, Zachary Garrett, Keith Rush, Jakub Konečný, Sanjiv Kumar, and H Brendan McMahan. Adaptive federated optimization. *arXiv preprint arXiv:2003.00295*, 2020.
- [4] Tian Li, Anit Kumar Sahu, Manzil Zaheer, Maziar Sanjabi, Ameet Talwalkar, and Virginia Smith. Federated optimization in heterogeneous networks. *Proceedings of Machine Learning and Systems*, 2:429–450, 2020.
- [5] Keith Bonawitz, Hubert Eichner, Wolfgang Grieskamp, Dzmitry Huba, Alex Ingerman, Vladimir Ivanov, Chloe Kiddon, Jakub Konečný, Stefano Mazzocchi, Brendan McMahan, et al. Towards federated learning at scale: System design. *Proceedings of Machine Learning and Systems*, 1:374–388, 2019.
- [6] Angelia Nedić, Dimitri P Bertsekas, and Vivek S Borkar. Distributed asynchronous incremental subgradient methods. *Studies in Computational Mathematics*, 8(C):381–407, 2001.
- [7] Horia Mania, Xinghao Pan, Dimitris Papailiopoulos, Benjamin Recht, Kannan Ramchandran, and Michael I Jordan. Perturbed iterate analysis for asynchronous stochastic optimization. *arXiv preprint arXiv:1507.06970*, 2015.
- [8] Alekh Agarwal and John C Duchi. Distributed delayed stochastic optimization. *Advances in neural information processing systems*, 24, 2011.
- [9] Konstantin Mishchenko, Francis Bach, Mathieu Even, and Blake Woodworth. Asynchronous sgd beats minibatch sgd under arbitrary delays. *arXiv preprint arXiv:2206.07638*, 2022.
- [10] Cong Xie, Sanmi Koyejo, and Indranil Gupta. Asynchronous federated optimization. *arXiv preprint arXiv:1903.03934*, 2019.

- [11] John Nguyen, Kshitiz Malik, Hongyuan Zhan, Ashkan Yousefpour, Mike Rabbat, Mani Malek, and Dzmitry Huba. Federated learning with buffered asynchronous aggregation. In *International Conference on Artificial Intelligence and Statistics*, pages 3581–3607. PMLR, 2022.
- [12] Dzmitry Huba, John Nguyen, Kshitiz Malik, Ruiyu Zhu, Mike Rabbat, Ashkan Yousefpour, Carole-Jean Wu, Hongyuan Zhan, Pavel Ustinov, Harish Srinivas, et al. Papaya: Practical, private, and scalable federated learning. *Proceedings of Machine Learning and Systems*, 4:814–832, 2022.
- [13] Jinhyun So, Ramy E Ali, Başak Güler, and A Salman Avestimehr. Secure aggregation for buffered asynchronous federated learning. *arXiv preprint arXiv:2110.02177*, 2021.
- [14] Anastasia Koloskova, Sebastian U Stich, and Martin Jaggi. Sharper convergence guarantees for asynchronous sgd for distributed and federated learning. *arXiv preprint arXiv:2206.08307*, 2022.
- [15] Sebastian U Stich and Sai Praneeth Karimireddy. The error-feedback framework: Better rates for sgd with delayed gradients and compressed communication. *arXiv preprint arXiv:1909.05350*, 2019.
- [16] Da Wang, Gauri Joshi, and Gregory Wornell. Using straggler replication to reduce latency in large-scale parallel computing. *ACM SIGMETRICS Performance Evaluation Review*, 43(3):7–11, 2015.
- [17] Can Karakus, Yifan Sun, Suhas Diggavi, and Wotao Yin. Straggler mitigation in distributed optimization through data encoding. *Advances in Neural Information Processing Systems*, 30, 2017.
- [18] Ganesh Ananthanarayanan, Ali Ghodsi, Scott Shenker, and Ion Stoica. Effective straggler mitigation: Attack of the clones. In *10th USENIX Symposium on Networked Systems Design and Implementation (NSDI 13)*, pages 185–198, 2013.
- [19] Tzu-Ming Harry Hsu, Hang Qi, and Matthew Brown. Measuring the effects of non-identical data distribution for federated visual classification. *arXiv preprint arXiv:1909.06335*, 2019.
- [20] Ruixuan Liu, Fangzhao Wu, Chuhan Wu, Yanlin Wang, Lingjuan Lyu, Hong Chen, and Xing Xie. No one left behind: Inclusive federated learning over heterogeneous devices. *Proceedings of the 28th ACM SIGKDD Conference on Knowledge Discovery and Data Mining*, 2022.
- [21] John Tsitsiklis, Dimitri Bertsekas, and Michael Athans. Distributed asynchronous deterministic and stochastic gradient optimization algorithms. *IEEE transactions on automatic control*, 31(9):803–812, 1986.
- [22] Qiyuan Wang, Qianqian Yang, Shibo He, Zhiguo Shui, and Jiming Chen. Asyncfed: Asynchronous federated learning with euclidean distance based adaptive weight aggregation. *arXiv preprint arXiv:2205.13797*, 2022.

- [23] Shuxin Zheng, Qi Meng, Taifeng Wang, Wei Chen, Nenghai Yu, Zhi-Ming Ma, and Tie-Yan Liu. Asynchronous stochastic gradient descent with delay compensation. In *International Conference on Machine Learning*, pages 4120–4129. PMLR, 2017.
- [24] Kangwook Lee, Maximilian Lam, Ramtin Pedarsani, Dimitris Papailiopoulos, and Kannan Ramchandran. Speeding up distributed machine learning using codes. *IEEE Transactions on Information Theory*, 64(3):1514–1529, 2017.
- [25] Amirhossein Reisizadeh, Isidoros Tziotis, Hamed Hassani, Aryan Mokhtari, and Ramtin Pedarsani. Straggler-resilient federated learning: Leveraging the interplay between statistical accuracy and system heterogeneity. *IEEE Journal on Selected Areas in Information Theory*, 3(2):197–205, 2022.
- [26] Zachary Charles, Zachary Garrett, Zhouyuan Huo, Sergei Shmulyian, and Virginia Smith. On large-cohort training for federated learning. *Advances in neural information processing systems*, 34:20461–20475, 2021.
- [27] Geoffrey Hinton, Oriol Vinyals, and Jeff Dean. Distilling the knowledge in a neural network. *arXiv preprint arXiv:1503.02531*, 2015.
- [28] Rohan Anil, Gabriel Pereyra, Alexandre Passos, Robert Ormandi, George E Dahl, and Geoffrey E Hinton. Large scale distributed neural network training through online distillation. *arXiv preprint arXiv:1804.03235*, 2018.
- [29] Neta Shoham, Tomer Avidor, Aviv Keren, Nadav Israel, Daniel Benditkis, Liron Mor-Yosef, and Itai Zeitak. Overcoming forgetting in federated learning on non-iid data. *ArXiv*, abs/1910.07796, 2019.
- [30] Boris T Polyak and Anatoli B Juditsky. Acceleration of stochastic approximation by averaging. *SIAM journal on control and optimization*, 30(4):838–855, 1992.
- [31] Jianyu Wang, Zachary Charles, Zheng Xu, Gauri Joshi, H Brendan McMahan, Maruan Al-Shedivat, Galen Andrew, Salman Avestimehr, Katharine Daly, Deepesh Data, et al. A field guide to federated optimization. *arXiv preprint arXiv:2107.06917*, 2021.
- [32] Gregory Cohen, Saeed Afshar, Jonathan Tapson, and Andre Van Schaik. Emnist: Extending mnist to handwritten letters. In *2017 International Joint Conference on Neural Networks (IJCNN)*, pages 2921–2926. IEEE, 2017.
- [33] Alex Krizhevsky, Geoffrey Hinton, et al. Learning multiple layers of features from tiny images. 2009.
- [34] The TensorFlow Federated Authors. Tensorflow federated stack overflow dataset, 2019. URL https://www.tensorflow.org/federated/api_docs/python/tff/simulation/datasets/stackoverflow/load_data.
- [35] Y. LeCun, Fu Jie Huang, and L. Bottou. Learning methods for generic object recognition with invariance to pose and lighting. In *Proceedings of the 2004 IEEE Computer Society Conference on Computer Vision and Pattern Recognition, 2004. CVPR 2004.*, volume 2, pages II–104 Vol.2, 2004. doi: 10.1109/CVPR.2004.1315150.

- [36] Kevin Jarrett, Koray Kavukcuoglu, Marc’Aurelio Ranzato, and Yann LeCun. What is the best multi-stage architecture for object recognition? In *2009 IEEE 12th International Conference on Computer Vision*, pages 2146–2153, 2009. doi: 10.1109/ICCV.2009.5459469.
- [37] Alex Krizhevsky. Convolutional deep belief networks on cifar-10. 2010. URL <https://api.semanticscholar.org/CorpusID:15295567>.
- [38] Kaiming He, X. Zhang, Shaoqing Ren, and Jian Sun. Deep residual learning for image recognition. *2016 IEEE Conference on Computer Vision and Pattern Recognition (CVPR)*, pages 770–778, 2015.
- [39] Sepp Hochreiter and Jürgen Schmidhuber. Long short-term memory. *Neural computation*, 9(8):1735–1780, 1997.
- [40] Jae Hun Ro, Ananda Theertha Suresh, and Ke Wu. FedJAX: Federated learning simulation with JAX. *arXiv preprint arXiv:2108.02117*, 2021.
- [41] Norman P. Jouppi, Cliff Young, Nishant Patil, David Patterson, Gaurav Agrawal, Raminder Bajwa, Sarah Bates, Suresh Bhatia, Nan Boden, Al Borchers, Rick Boyle, Pierre-luc Cantin, Clifford Chao, Chris Clark, Jeremy Coriell, Mike Daley, Matt Dau, Jeffrey Dean, Ben Gelb, Tara Vazir Ghaemmaghami, Rajendra Gottipati, William Gulland, Robert Hagmann, C. Richard Ho, Doug Hogberg, John Hu, Robert Hundt, Dan Hurt, Julian Ibarz, Aaron Jaffey, Alek Jaworski, Alexander Kaplan, Harshit Khaitan, Daniel Killebrew, Andy Koch, Naveen Kumar, Steve Lacy, James Laudon, James Law, Diemthu Le, Chris Leary, Zhuyuan Liu, Kyle Lucke, Alan Lundin, Gordon MacKean, Adriana Maggiore, Maire Mahony, Kieran Miller, Rahul Nagarajan, Ravi Narayanaswami, Ray Ni, Kathy Nix, Thomas Norrie, Mark Omernick, Narayana Penukonda, Andy Phelps, Jonathan Ross, Matt Ross, Amir Salek, Emad Samadiani, Chris Severn, Gregory Sizikov, Matthew Snelham, Jed Souter, Dan Steinberg, Andy Swing, Mercedes Tan, Gregory Thorson, Bo Tian, Horia Toma, Erick Tuttle, Vijay Vasudevan, Richard Walter, Walter Wang, Eric Wilcox, and Doe Hyun Yoon. In-datacenter performance analysis of a tensor processing unit. In *Proceedings of the 44th Annual International Symposium on Computer Architecture*, ISCA ’17, page 1–12, New York, NY, USA, 2017. Association for Computing Machinery. ISBN 9781450348928. doi: 10.1145/3079856.3080246. URL <https://doi.org/10.1145/3079856.3080246>.
- [42] Shagun Sodhani, Olivier Delalleau, Mahmoud Assran, Koustuv Sinha, Nicolas Ballas, and Michael Rabbat. A closer look at codistillation for distributed training, 2021.
- [43] Joachim Houyon, Anthony Cioppa, Yasir Ghunaim, Motasem Alfarra, Anaïs Halin, Maxim Henry, Bernard Ghanem, and Marc Van Droogenbroeck. Online distillation with continual learning for cyclic domain shifts, 2023.
- [44] Lucas Beyer, Xiaohua Zhai, Amélie Royer, Larisa Markeeva, Rohan Anil, and Alexander Kolesnikov. Knowledge distillation: A good teacher is patient and consistent. In *2022 IEEE/CVF Conference on Computer Vision and Pattern Recognition (CVPR)*, pages 10915–10924, 2022. doi: 10.1109/CVPR52688.2022.01065.

- [45] Mitchell Wortsman, Gabriel Ilharco, Samir Ya Gadre, Rebecca Roelofs, Raphael Gontijo-Lopes, Ari S Morcos, Hongseok Namkoong, Ali Farhadi, Yair Carmon, Simon Kornblith, et al. Model soups: averaging weights of multiple fine-tuned models improves accuracy without increasing inference time. In *International Conference on Machine Learning*, pages 23965–23998. PMLR, 2022.
- [46] Virat Shejwalkar, Arun Ganesh, Rajiv Mathews, Om Thakkar, and Abhradeep Thakurta. Recycling scraps: Improving private learning by leveraging intermediate checkpoints. *ArXiv*, abs/2210.01864, 2022. URL <https://api.semanticscholar.org/CorpusID:252715601>.
- [47] Jiawei Du, Daquan Zhou, Jiashi Feng, Vincent Y. F. Tan, and Joey Tianyi Zhou. Sharpness-aware training for free. *ArXiv*, abs/2205.14083, 2022. URL <https://api.semanticscholar.org/CorpusID:249152070>.
- [48] Pavel Izmailov, Dmitrii Podoprikin, T. Garipov, Dmitry P. Vetrov, and Andrew Gordon Wilson. Averaging weights leads to wider optima and better generalization. In *Conference on Uncertainty in Artificial Intelligence*, 2018. URL <https://api.semanticscholar.org/CorpusID:3833416>.
- [49] Timur Garipov, Pavel Izmailov, Dmitrii Podoprikin, Dmitry P Vetrov, and Andrew G Wilson. Loss surfaces, mode connectivity, and fast ensembling of dnns. *Advances in neural information processing systems*, 31, 2018.
- [50] Felix Draxler, Kambis Veschgini, Manfred Salmhofer, and Fred Hamprecht. Essentially no barriers in neural network energy landscape. In *International conference on machine learning*, pages 1309–1318. PMLR, 2018.
- [51] Jonathan Frankle, Gintare Karolina Dziugaite, Daniel Roy, and Michael Carbin. Linear mode connectivity and the lottery ticket hypothesis. In *International Conference on Machine Learning*, pages 3259–3269. PMLR, 2020.
- [52] Sean Augenstein, Andrew Hard, Lin Ning, Karan Singhal, Satyen Kale, Kurt Partridge, and Rajiv Mathews. Mixed federated learning: Joint decentralized and centralized learning, 2022.
- [53] David Leroy, Alice Coucke, Thibaut Lavril, Thibault Gisselbrecht, and Joseph Dureau. Federated learning for keyword spotting. In *ICASSP 2019-2019 IEEE International Conference on Acoustics, Speech and Signal Processing (ICASSP)*, pages 6341–6345. IEEE, 2019.
- [54] Andrew Hard, Kurt Partridge, Neng Chen, Sean Augenstein, Aishanee Shah, Hyun Jin Park, Alex Park, Sara Ng, Jessica Nguyen, Ignacio Lopez Moreno, et al. Production federated keyword spotting via distillation, filtering, and joint federated-centralized training. *arXiv preprint arXiv:2204.06322*, 2022.
- [55] Vanessa Frias-Martinez and Jesus Virseda. On the relationship between socio-economic factors and cell phone usage. In *Proceedings of the fifth international conference on information and communication technologies and development*, pages 76–84, 2012.

- [56] Jessica E Steele, Carla Pezzulo, Maximilian Albert, Christopher J Brooks, Elisabeth zu Erbach-Schoenberg, Siobhán B O'Connor, Pål R Sundsøy, Kenth Engø-Monsen, Kristine Nilsen, Bonita Graupe, et al. Mobility and phone call behavior explain patterns in poverty at high-resolution across multiple settings. *Humanities and Social Sciences Communications*, 8(1):1–12, 2021.

A Algorithm details for FARE-DUST and FeAST-on-MSG

A.1 Motivation

This work began with applying small modifications (EMA, knowledge distillation) to `FedBuff` for the purpose of improving the representation of straggler clients in the learned model. These techniques are introduced in Section 2.1, and observations are summarized in Appendix B. Each technique provided improvements over the baseline `FedBuff` algorithm, as summarized in Tables 20, 22, 23, 24, and 25. These incremental benefits motivated the development of new algorithms built around three concepts:

1. knowledge distillation to incorporate stale updates,
2. EMA and model averaging to combine models trained on different data partitions,
3. application of gradients to mismatched network weights.

We provide some background and motivation for each of these concepts below.

Distillation Co-distillation [28] originally used distillation regularization to overcome the limitations of scaling batch size alone for parallel training on massive datasets. Sodhani et al. [42] hinted that co-distillation could be used to speed up federated training. It was therefore reasonable to suspect that distillation might bring data parallelism benefits to the asynchronous FL regime.

There was also evidence that distillation could transfer domain knowledge from a teacher to a student even for domains that were absent from the distillation training dataset. Houyon et al. [43] demonstrated that distillation could be used to mitigate cyclical domain shifts. And Beyer et al. [44] showed that student models could learn classes from the soft labels of a teacher, even when those classes were not present in the student’s training data.

These prior works led to our hypothesis that, *if stale updates were considered as a data class of their own, knowledge distillation from a stale teacher could be used to impart knowledge of the stale class to faster clients in FL*. The strong performance of `FARe-DUST` in experiments (high straggler accuracy, total accuracy, and reduced training latency) supports this hypothesis.

EMA and model averaging Model averaging has shown promising results when combining models fine-tuned with different hyper-parameters or data subsets [45], combining models trained with noisy gradients with varying data distributions [46], and as an effective way of approximating the sharpness of the loss [47]. Prior works suggest that model averaging can result in wider optima and better generalization [48].

A similar line of work on mode connectivity [49, 50, 51] has shown that the optima of SGD-trained neural networks are connected by smooth curves over which accuracy and loss are nearly constant. In particular, Frankle et al. [51] demonstrated the existence of linear mode connectivity for checkpoints derived from a recent common ancestor checkpoint. This is quite similar to the finding of Wortsman et al. [45], which found that models could be averaged effectively as long as they shared a common initial checkpoint for fine-tuning.

The averaging and mode connectivity literature motivated the application of EMA and model averaging to the stale weight update problem in this work. The wider optima and better generalization provided by EMA would be beneficial to FL, since models learned on a subset of clients must generalize to unseen clients. Furthermore, the wider optima provided by EMA would likely be more amenable to averaging across multiple time steps. Linear mode connectivity suggested that extremely stale weight updates could still be averaged with more recent global models, since straggler weight updates would share a common ancestor with more recent checkpoints created by fast FL clients.

Mismatched gradients The model averaging and mode connectivity works also led us to a hypothesis that *it might also be possible to transfer gradients from one model to another in certain cases*. Particularly for two models with mode connectivity or wide minima, transferring gradients associated with one set of weights to another set of weights could effectively transfer knowledge about the learned data. In fact, gradient transfer has been used in Augenstein et al. [52] to train models on disjoint datasets.

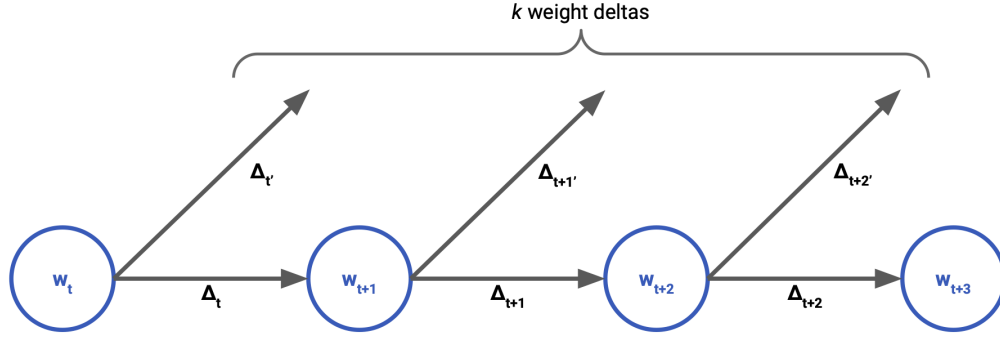
Motivation for FARE-DUST Both of our algorithms utilize straggler aggregation, in which straggler client weight updates $\Delta_{t'}$ continue to be aggregated by the server even after FL round t is completed and the fast client updates Δ_t are applied to advance the global model: $w_{t+1} \leftarrow w_t - \frac{\eta_g}{B} \Delta_t$. The FARE-DUST algorithm also relies on the three techniques of mismatched gradients, distillation for knowledge transfer, and EMA.

- Mismatched gradients: teacher networks are constructed by applying the straggler weight deltas ($\Delta_{t'}$ to the *most recent global model* rather than the global model which was used to compute the gradients.
- Distillation for knowledge transfer: the teachers formed from mismatched gradients are used for distillation regularization in subsequent training rounds. Straggler client knowledge from the mismatched gradients thus gets distilled into all clients in the current round.
- EMA: the final model is produced by applying EMA to the main model weights $(w_T, w_{T-1}, w_{T-2}, \dots)$.

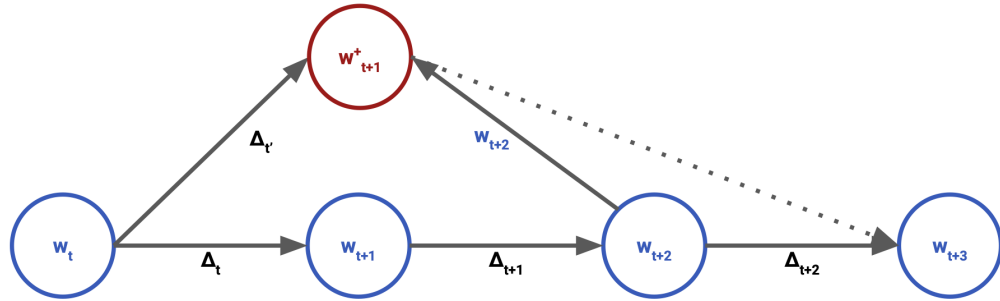
Figure 4 illustrates the novel aspects of the FARE-DUST algorithm.

Motivation for FeAST-on-MSG In addition to straggler aggregation, the FeAST-on-MSG algorithm uses the techniques of mismatched gradients and EMA.

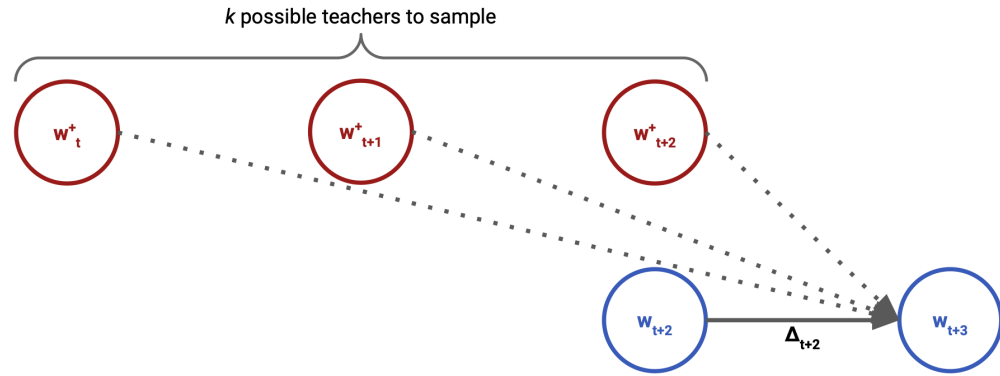
- Mismatched gradients: FeAST-on-MSG applies the straggler weight deltas ($\Delta_{t'}$ to the auxiliary model weights a_t , as well as to the corresponding main global model w_t .
- EMA: the auxiliary model a_{t+1} is formed using weight averaging of the straggler-updated model weights w_t^+ and the previous auxiliary model with the mismatched gradient applied $(a_t - \frac{\eta_a}{B_t^+} \Delta_t^+)$.



(a) **Stale gradient accumulation.** Historical weight deltas $\Delta_{t'}, \Delta_{t+1'}, \Delta_{t+2'}, \Delta_{t+3'}, \dots$ are maintained for up to k prior FL rounds behind the primary weight branch. Updates from straggler clients continue to accumulate in these weight deltas even after the primary weight branch ($w_t, w_{t+1}, w_{t+2}, \dots$) has advanced.



(b) **Teacher network creation.** For a given client and given FL training round, an historical weight delta is selected at random from the k possible choices to construct a teacher network. In this diagram, $\Delta_{t'}$ is selected and applied to the current global model w_{t+2} to form the teacher network w_{t+1}^+ via the update: $w_{t+1}^+ = w_{t+2} - (\frac{\eta_g}{B_t^+})\Delta_{t'}$.



(c) **Stale teacher distillation.** Each client in each round is randomly assigned one of the possible k historical teachers for distillation regularization. In this example, the initial global model w_{t+2} is sent to each client along with one of the historical teachers ($w_t^+, w_{t+1}^+, w_{t+2}^+$). A new global model, w_{t+3} , is formed by aggregating the local client updates that were formed by training with the standard supervised and distillation regularization objectives. After T rounds, w_T (or the EMA of w_T, w_{T-1}, \dots) is returned as the final model.

Figure 4: A diagram of the three main components of FARE-DUST: stale gradient accumulation (Figure 4a), teacher network creation (Figure 4b), and stale teacher distillation (Figure 4c).

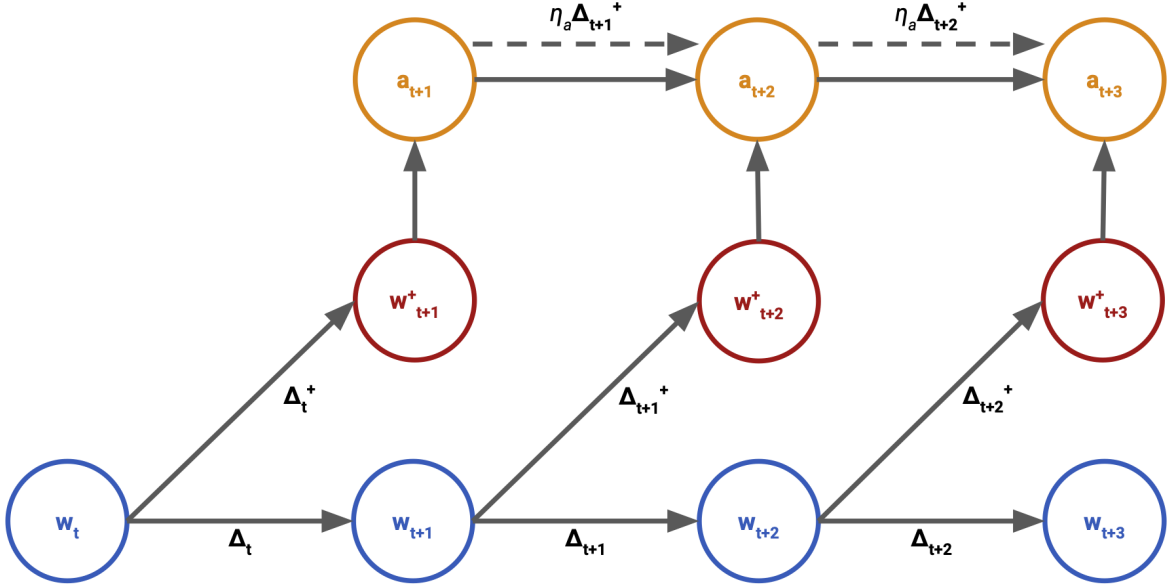


Figure 5: A visual diagram of the FeAST-on-MSG algorithm. The primary weight branch $(w_t, w_{t+1}, w_{t+2}, \dots)$ is advanced as usual for FedAvg. However, additional straggler updates are also allowed to accumulate for each checkpoint as they are received by the server $(\Delta_t^+, \Delta_{t+1}^+, \Delta_{t+2}^+, \dots)$, up to a maximum wait time τ_{\max} . Once the maximum wait time has elapsed, an historical checkpoint is formed using the update: $w_{t+1}^+ = w_t - (\frac{\eta_g}{B_t^+})\Delta_t^+$. Historical checkpoints $w_{t+1}^+, w_{t+2}^+, w_{t+3}^+, \dots$ are formed as the maximum wait times for each round elapse. An auxiliary branch $(a_{t+1}, a_{t+2}, a_{t+3}, \dots)$ is advanced based on the historical checkpoints and stale gradients: $a_{t+1} = \beta(a_t - \frac{\eta_a}{B_t^+}\Delta_t^+) + (1 - \beta)w_{t+1}^+$. After a maximum of T training rounds, a_T is returned as the final model.

Figure 5 illustrates the components of the FeAST-on-MSG algorithm. Equation 2 also provides the exact FeAST-on-MSG update formula. There are two special cases for the algorithm. First, when $\eta_a = 0$ with $a_0 = w_0^+ = w_0$, the auxiliary model update is just an EMA of the past models with decay β . Second, when $\eta_a = \eta_g$, the auxiliary model update is essentially a gradient step on a weighted average of the current auxiliary and global models.

Our empirical evaluation of FeAST-on-MSG validates that *model averaging and mismatched gradient transfer can successfully transmit information between models trained on different data partitions*.

A.2 Pseudo-code

This section provides pseudo-code for the algorithms presented in Section 2. The server and client computation pseudo-code for FARE-DUST are shown in Algorithm 1 and Algorithm 3, respectively. The FeAST-on-MSG server computation pseudo-code is shown in Algorithm 2.

Algorithm 1 FARE-DUST: server-side

Input: client cohort size B , server learning rate η_g , client learning rate η_l , maximum number of teachers k , distillation strength parameter ρ , and EMA decay β .

```
1: Initialize:  $w_0 \in \mathbb{R}^d$ ,  $t \leftarrow 0$ , Deltas = {}
2: while  $t \leq T$  do
3:   Sample a subset  $\mathcal{C}_t$  of size  $B_t = |\mathcal{C}_t|$  clients.
4:    $b_t \leftarrow 0$ ,  $\Delta_t \leftarrow 0$ .
5:   for each client  $c \in \mathcal{C}_t$  in parallel do
6:     Sample uniformly  $\Delta_{\text{teacher}}^c$  from Deltas.
7:      $w_{\text{teacher}}^c \leftarrow w_t - \frac{\eta_g}{B_{\text{teacher}}^c} \Delta_{\text{teacher}}^c$ .
8:     Run FARE-DUSTclient( $w_t, w_{\text{teacher}}^c$ ).
9:   end for
10:  while  $b_t < B$  do
11:    if receive client  $c \in \mathcal{C}_t$  update then
12:       $\Delta_t \leftarrow \Delta_t + \Delta_t^c$ ,  $b_t \leftarrow b_t + 1$ .
13:    end if
14:  end while
15:   $w_{t+1} \leftarrow w_t - \frac{\eta_g}{B} \Delta_t$ ,  $t \leftarrow t + 1$ .
16:   $\Delta_t \leftarrow 0$ ,  $b_t \leftarrow 0$ 
17:  Add  $(\Delta_t, b_t)$  to the set Deltas.
18:  if receive client  $c \in \mathcal{C}_{t'}$ ,  $t' \leq t$  update then
19:     $\Delta_{t'} \leftarrow \Delta_{t'} + \Delta_{t'}^c$ ,  $b_{t'} \leftarrow b_{t'} + 1$ .
20:  end if
21:  if  $|\text{Deltas}| > k$  then
22:     $w_{t-k-1} \leftarrow w_{t-k-1} - \frac{\eta_g}{b_{t-k-1}} \Delta_{t-k-1}$ .
23:    Remove  $\Delta_{t-k-1}$  from Deltas.
24:  end if
25: end while
```

Output: Global model: $\text{EMA}_\beta(w_1, \dots, w_T)$.

B Additional Observations

FARe-DUST FARE-DUST was the most consistently high-performing algorithm across tasks, providing an excellent trade-off between total training time, straggler accuracy, and total accuracy. In the EMNIST + **per-domain per-example** experiments (Figure 15a), FARE-DUST achieved the best trade-off of straggler accuracy and total accuracy of any algorithm by a significant margin (FeAST-on-MSG had better straggler accuracy, at the cost of much lower total accuracy), while also converging quickly. In experiments with CIFAR-100 and the **per-example** client latency model, FARE-DUST again had the best combination of straggler accuracy and total accuracy (Figure 17a). And with the **per-domain per-example** client latency scenario, FARE-DUST and FedAdam were tied for best accuracy trade-offs (Figure 19a). However, FARE-DUST was also $2.5\times$ faster in terms of wall-clock time than FedAdam in this setting (Figure 19b). Finally, on the StackOverflow task with the **per-domain per-example**

Algorithm 2 FeAST-on-MSG: server-side

Input: cohort size B , server learning rate η_g , auxiliary learning rate η_a , client learning rate η_l , maximum wait time τ_{\max} , and EMA decay β .

- 1: **Initialize:** $w_0 \in \mathbb{R}^d$, $t \leftarrow 0$, $a_0 \leftarrow w_0$
- 2: **while** $t \leq T$ **do**
- 3: Sample a subset \mathcal{C}_t of B_t clients and run client computations.
- 4: $b_t \leftarrow 0$, $\Delta_t \leftarrow 0$.
- 5: Reset and record `elapsed_time`.
- 6: **while** $b_t < B$ **do**
- 7: Receive client $c \in \mathcal{C}_t$ update.
- 8: $\Delta_t \leftarrow \Delta_t + \Delta_t^c$, $b_t \leftarrow b_t + 1$.
- 9: **end while**
- 10: $w_{t+1} \leftarrow w_t - \frac{\eta_g}{b_t} \Delta_t$, $t \leftarrow t + 1$.
- 11: $\Delta_t^+ \leftarrow \Delta_t$.
- 12: **while** `elapsed_time` $\leq \tau_{\max}$ **do**
- 13: Receive client $c \in \mathcal{C}_t$ update.
- 14: $\Delta_t^+ \leftarrow \Delta_t^+ + \Delta_t^c$, $b_t \leftarrow b_t + 1$.
- 15: **end while**
- 16: $w_{t+1}^+ \leftarrow w_t - \frac{\eta_g}{b_t} \Delta_t^+$.
- 17: $a_{t+1} \leftarrow \beta (a_t - \frac{\eta_a}{b_t} \Delta_t^+) + (1 - \beta) w_{t+1}^+$.
- 18: **end while**

Output: Global model: a_T .

client latency model, FARE-DUST achieved the 2nd highest straggler accuracy and total accuracy (Figure 23a), but was 10× faster than FedAdam, which had the highest straggler accuracy (Figure 23b). Generally speaking, FARE-DUST was faster than FedAdam without over-selection, and had higher total and straggler accuracy than FedBuff or FedAdam with over-selection. FARE-DUST performed particularly well in the `per-domain per-example` latency scenario, indicating that it was able to learn very effectively from clients that were significantly delayed.

FeAST-on-MSG FeAST-on-MSG also provided high straggler and total accuracy across most tasks and provided a good trade-off between training time and accuracy. Generally

Algorithm 3 FARE-DUST_{client}: client-side

Input: model w , teacher model w_{teacher} , local iterations T_l , loss function F_i , distillation loss ψ , distillation parameter ρ , and learning rate η_l .

- 1: **Initialize:** $w_0^i \leftarrow w$.
- 2: **for** $j = 0, \dots, T_l - 1$ **do**
- 3: $w_{j+1}^i \leftarrow w_j^i - \eta_l \nabla_{w_j^i} (F_i(w_j^i) + \rho \psi(w_j^i, w_{\text{teacher}}))$
- 4: **end for**

Output: Local update: $\Delta^i = w_{T_l}^i - w$.

speaking, **FeAST-on-MSG** was comparable in terms of total training time with **FARe-DUST**, faster than **FedAdam** without over-selection, and had higher accuracy than **FedBuff**. In experiments with EMNIST and the **per-example** client latency model (Table 20), **FeAST-on-MSG** tied with **FedAdam** over-selection for the best straggler accuracy and total accuracy while being significantly faster. For StackOverflow experiments with the **per-example** client latency scenario, **FeAST-on-MSG** achieved the best trade-off between straggler accuracy and total accuracy. It was second in straggler accuracy only to **FedAdam** (Figure 21a), and was $10\times$ faster in terms of wall-clock time (Figure 21b). And in StackOverflow experiments with the **per-domain per-example** client latency model, **FeAST-on-MSG** was second only to **FARe-DUST** in terms of the accuracy-time trade-off (Figure 23b). However, **FeAST-on-MSG** had a drawback: it was susceptible to over-tuning on straggler accuracy at the expense of total accuracy. Evidence of this can be seen in the EMNIST (Figure 15a) and CIFAR-100 (Figure 19a) experiments with the **per-domain per-example** client latency scenario, in which **FeAST-on-MSG** achieved unrivaled straggler accuracies of 99.3% and 58.6%, respectively, while also having lower total accuracy than all other algorithms.

Large values for $\kappa = (\eta_a/\eta_g)$, which controls the auxiliary learning rate, help explain why **FeAST-on-MSG** over-fits to straggler accuracy in these two cases (see Tables 18 and 19). When $\kappa = 0$, **FeAST-on-MSG** reduces to EMA on the past models. Larger values of κ , on the other hand, give greater weight to the mismatched gradient Δ_t^+ applied to the auxiliary model a_t . Thus, κ has an important role in regulating the trade-off between straggler client accuracy and non-straggler client accuracy for **FeAST-on-MSG**.

FedAdam When used with over-selection, **FedAdam** provided excellent trade-offs between straggler accuracy, total accuracy, and training time in the **per-example** client latency scenario. For example, **FedAdam** with over-selection achieved the highest straggler accuracy with the **per-example** client latency scenario for EMNIST (Table 20) and CIFAR-100 (Table 22). This result makes sense because straggler clients in this latency scenario were distinguished by data volume rather than data class. However, **FedAdam** with over-selection fared less well under the **per-domain per-example** client latency scenario. When using over-selection, straggler clients with straggler data were never aggregated into the global model. And without over-selection, **FedAdam** was significantly slower to converge than other algorithms. This can be observed in the **per-domain per-example** client latency model results with EMNIST (Table 21) and CIFAR-100 (Table 23)

FedBuff **FedBuff** provided the fastest convergence by far on EMNIST and CIFAR-100, but yielded lower total accuracy (Figures 14b and 18b) and straggler accuracy (Figures 14a and 18a). For the StackOverflow task, **FedBuff** was actually slower than the synchronous algorithms with over-selection (Figure 20b). This was due to the fact that **FedBuff** was unstable on the StackOverflow tasks when run with small buffer sizes. Tuning experiments identified a buffer size of 50 along with a max concurrency of 100 as the most stable and accurate configuration. For comparison, **FedBuff** worked with a buffer size of 20 and max concurrency of 60 for CIFAR-100, and a buffer size of 20 with a max concurrency of 100 for EMNIST. It should also be noted that, even after tuning buffer size, max concurrency, and learning rates, the **FedBuff** algorithm accuracy was highly variable from one round to the

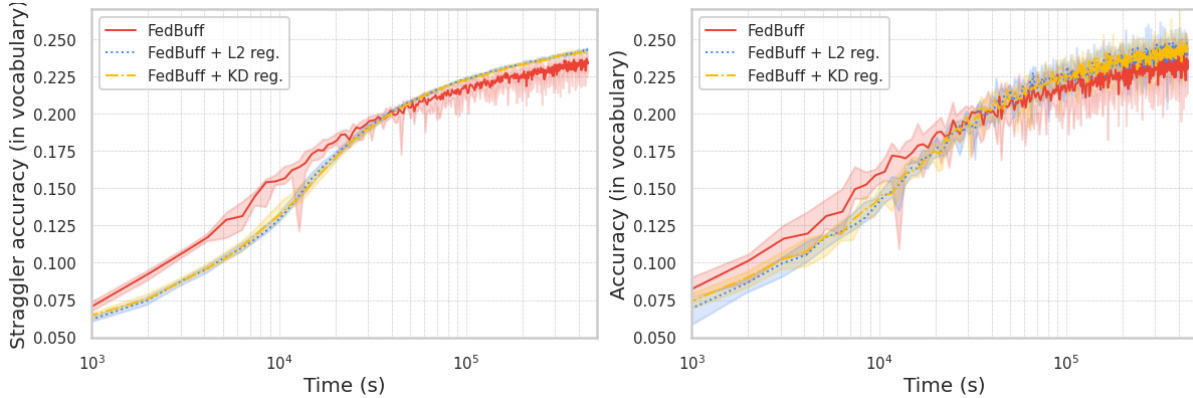


Figure 6: Straggler accuracy (left) and total accuracy (right) as a function wall clock training time for StackOverflow with the `per-domain per-example` client latency scenario. The training curves for the `FedBuff` algorithm are shown with and without distillation and proximal L_2 regularization.

next in every task. We chose to explore regularization techniques for the purpose of reducing the performance variance in `FedBuff`.

Regularized FedBuff We experimented with regularized versions of the `FedBuff` algorithm including distillation regularization and proximal L_2 regularization. Figure 6 compares accuracy for these variants of `FedBuff` on the StackOverflow task with the `per-domain per-example` client latency model. Both forms of regularization lead to improved total accuracy and straggler accuracy. For the most part, these regularization techniques were beneficial in terms of accuracy (and reduced variance in performance) across tasks and latency models. We hypothesized that both techniques were able to reduce client drift for clients in the buffer, even when the client computations originated from different time steps.

FedBuff with EMA Figure 7 compares `FedBuff` with EMA ($\beta = 0.99$) and without EMA on the model weights, for the EMNIST task. While the median straggler accuracy and total accuracy were comparable in both latency scenarios, the variance of the performance was significantly lower when using EMA.

Adaptive FedBuff Figure 7 also compares `FedBuff` with SGD as the server optimizer (default) and with Adam as the server optimizer. The results show that Adam significantly improved the straggler accuracy and total accuracy of `FedBuff`. Unfortunately, we did not have time to provide results with Adam as the server optimizer for all tasks in this work. However, the results suggested that, as with synchronous FL and `FedAdam`, asynchronous FL algorithms might benefit significantly from adaptive server optimizers.

Impact of over-selection Over-selection significantly sped up `FedAvg` and `FedAdam`, and even boosted accuracy on the `per-example` client latency tasks (Figure 8a and 8b). Over-selection was incredibly useful when there were no data domain differences between fast

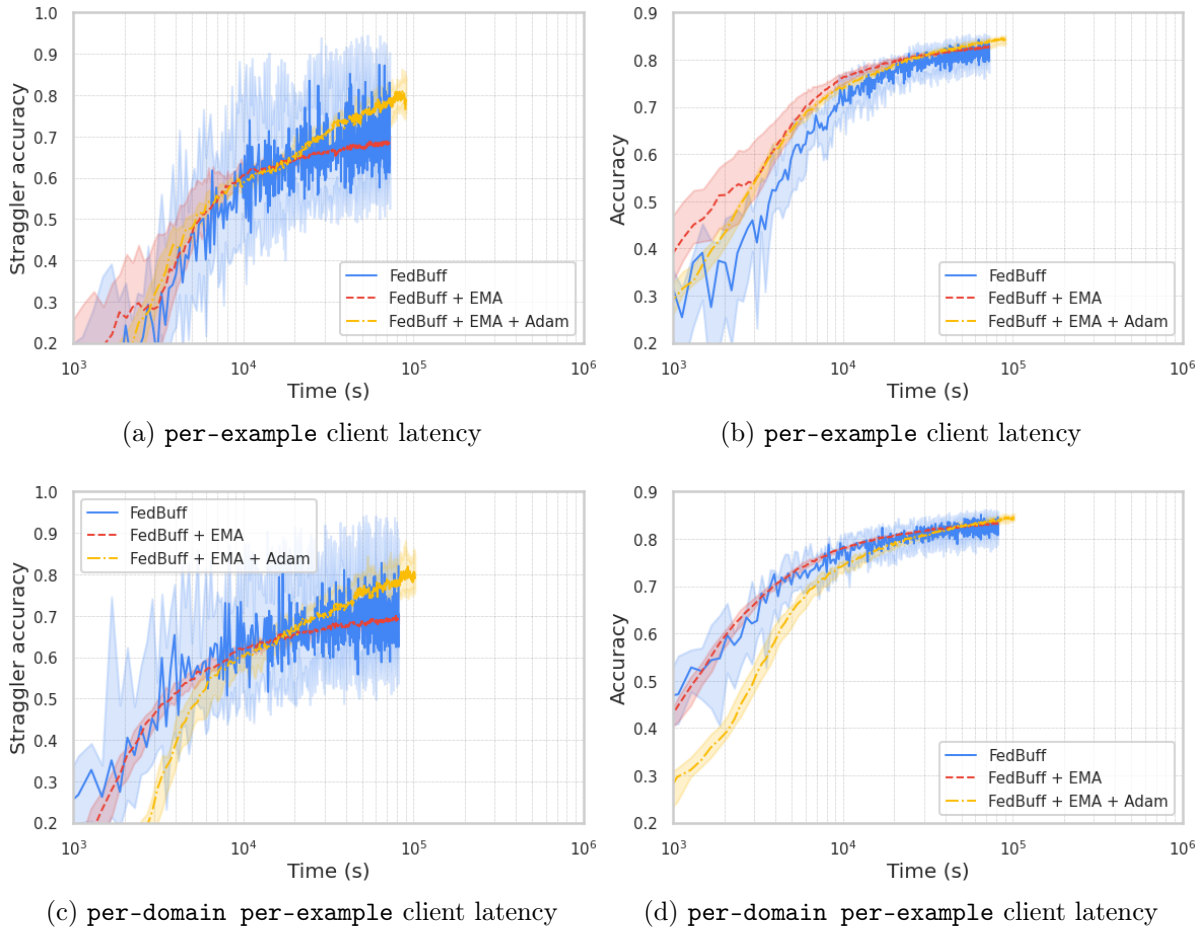


Figure 7: Straggler accuracy (left) and total accuracy (right) as a function wall clock training time for EMNIST with the **per-example** client latency (top) and **per-domain per-example** client latency scenario (bottom). The training curves for the FedBuff algorithm are shown with and without EMA and the Adam server optimizer.

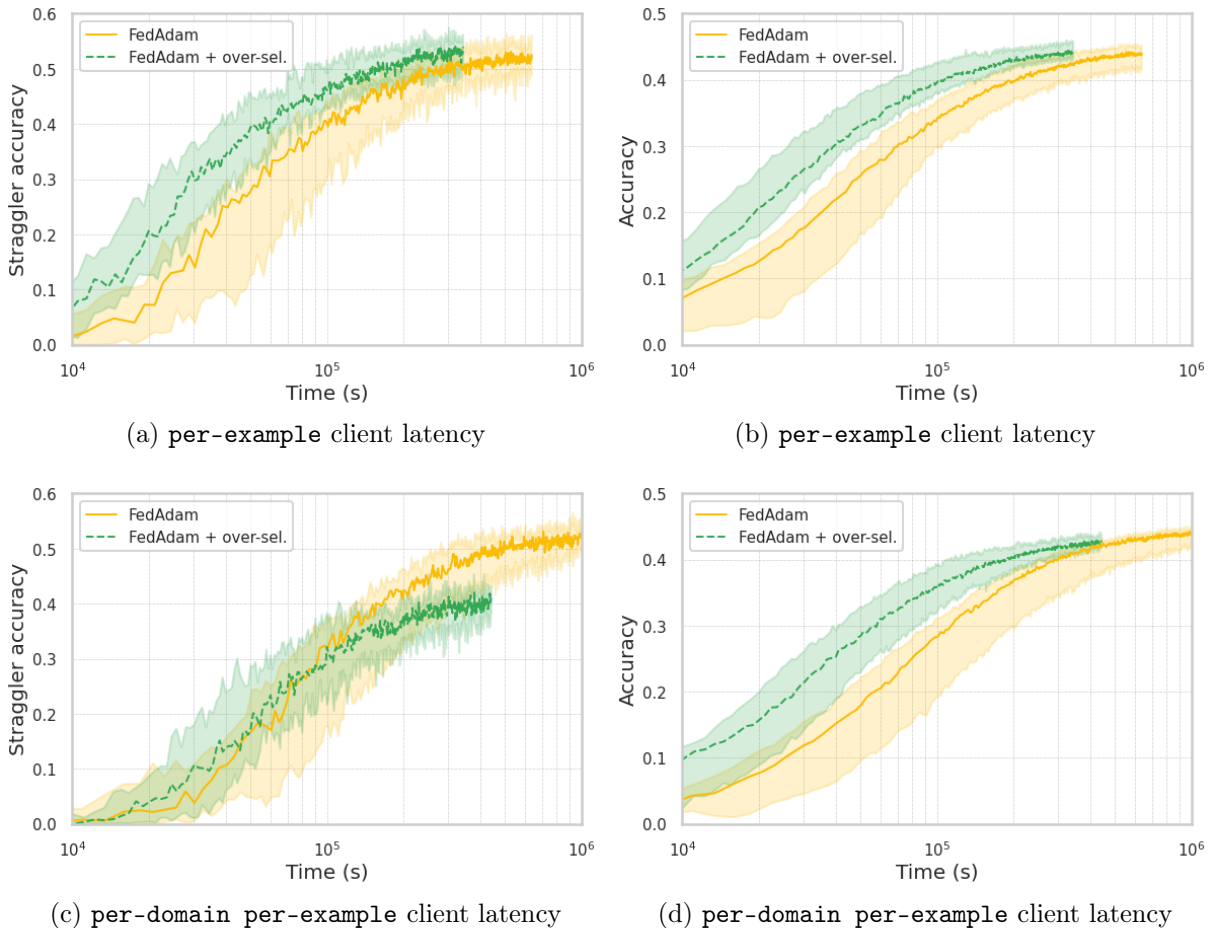


Figure 8: Straggler accuracy (left) and total accuracy (right) as a function wall clock training time for CIFAR-100 with the **per-example** client latency (top) and **per-domain per-example** client latency scenario (bottom). The training curves for the FedAdam algorithm are shown with and without over-selection.

and straggler clients (only differences in data volume or other random factors). However, over-selection typically led to worse straggler accuracy and total accuracy on the **per-domain per-example** client latency task (Figure 8c and 8d). While fast and slow clients had the same data distribution in the **per-example** scenario, that was not the case for the **per-domain per-example** client latency scenario. In that setting, all of the clients with straggler data domains (0-4 for EMNIST, “vehicles 1” and “vehicles 2” for CIFAR-100, “math” and “c + +” for StackOverflow) were dropped from the training round due to high latency. In tuning experiments, we observed that the best trade-offs were achieved when the over-selection percentage corresponded roughly to the prevalence of straggler clients in the total population.

Time-limited client computation Limiting the client computations by time rather than the number of local epochs or local steps of SGD significantly sped up training for FedAvg. In the **per-example** client latency scenario, the speed-up often came with no reduction in accuracy (Table 20). However, in the **per-domain per-example** latency scenario, the

speed-up came at the price of reduced straggler accuracy (Table 21). The difference was likely due to the fact that, in the `per-domain per-example` latency scenario, fewer training steps were performed on slow clients. This inevitably biased the learned models towards the fast clients that lacked straggler data domains. Furthermore, the trade-off between latency and accuracy was not competitive with other modifications to FL algorithms such as over-selection. Irreducible latency factors such as the communication time and system overhead were always present, and could be fully accounted for in the time limit applied by clients. While experiments were only performed for the `FedAvg` algorithm, the technique could be coupled with any of the other synchronous or asynchronous algorithms discussed in this work.

Accuracy vs. training time trade-off Each algorithm has multiple parameters that adjust the trade-off between straggler accuracy, total accuracy, and total training time. To start with, the over-selection fraction for `FedAvg`, `FedAdam`, `FARe-DUST`, and `FeAST-on-MSG` could be increased to reduce training time, at the expense of straggler accuracy in the `per-domain per-example` latency scenario. For `FedBuff`, the buffer size (B) and maximum number of concurrent clients (χ) could be tuned to affect the accuracy-time trade-off. Larger B typically led to smoother convergence and higher accuracy, but slower training. On the other hand, larger values of χ produced faster training but resulted in extremely high variance in model accuracy. Client computation time limits could also be used in conjunction with any algorithm to adjust the accuracy-time trade-off. However, experiments showed that other techniques such as over-selection provided better trade-offs in most tasks. Finally, the maximum wait time, τ_{\max} , for the `FeAST-on-MSG` algorithm affected the training time and straggler accuracy. τ_{\max} simply added a constant factor to the total training time. Even when waiting for 99% of clients from all rounds, this amounted to a negligible increase in total training time. We observed that straggler accuracy increased with increasing τ_{\max} .

StackOverflow experiments `FedAdam` both with and without over-selection performed surprisingly well in experiments with the StackOverflow dataset. `FedAdam` achieved the highest straggler accuracy for StackOverflow with both client latency models (Table 24 and 25), though it required an order of magnitude longer training time than the algorithms proposed in this work. `FedAdam` with over-selection, meanwhile, had comparable training time to `FeAST-on-MSG` and `FARe-DUST` with a straggler accuracy that was only modestly lower. We believe that the strong performance of the baseline algorithms on StackOverflow is due to the similarity of data domains for straggler clients and standard clients. Recall that straggler clients corresponded to users who submitted questions and answers with the “math” and “c + +” tags, while the standard clients corresponded to all other clients. Despite this tag separation, the language modeling tasks for the two groups of users were quite similar. There would be a high degree of overlap between the semantics and vocabularies of the two user domains, and no explicit output class separations. Thus, it is reasonable to expect models trained on standard clients in this setting could also generalize to straggler clients. This is in contrast to the EMNIST and CIFAR-100 datasets, where standard and straggler clients featured explicit output class partitions.

Table 5: The client upload time, client train time, and system constant time as measured in a real-world application of FL for keyword spotting.

Percentile	Upload [s]	Train [s]	System [s]
50%	5.1	26	24
75%	7.6	86	33
95%	9.6	180	36
99%	15	270	40

C Measurements from real-world FL

Several real-world observations of FL client latency have been published previously. For example, Wang et al. [31] estimated values for the parameters described in Section 3.1. That work quoted average values in some cases and 90th percentile values for communication costs. Straggler modeling was highlighted as a direction for future work.

Client execution time histograms were presented in Huba et al. [12]. Execution times spanned 3 orders of magnitude in the examples provided. The mean round duration was also $21\times$ larger than the mean client execution time. Two factors were conflated in this result: the number of examples per device, and the per-example training time. Histograms of the number of examples per client also spanned 3 orders of magnitude. This suggested that variance in the number of training steps explained the latency distribution.

We measured client latencies in a production keyword spotting task similar to those presented in Leroy et al. [53] and Hard et al. [54]. Percentile values for the client upload time, client train time, and the system constant time are shown in Table 5. Measurements were taken during peak training hours for a model consisting of approximately 300,000 parameters with a communication payload of 1.3MB. Approximately 600 examples were processed by the median client. As with the measurements from Huba et al. [12], the train time quoted here conflates the number of steps per client and the per-step execution times. However, based on the number of client steps for the tasks, it was possible to infer that per-step computation times varied by $5 - 10\times$ between the median and 99th percentile.

Latency component distributions vary with the model size, the federated computations, the client device types, and even the time of day. Nevertheless, some general observations can be made from the real-world examples. First, total training time for clients can vary by 1-2 orders of magnitude across a federated population. And second, all sources of client latency have large differences between the median and 99th percentile values. In the examples shown here, training time was a more dominant factor than communication time. But the trade-off would change for different model sizes or numbers of local client training steps.

D Limitations

In this work, we compared the capacity of multiple FL algorithms to learn from straggler clients. The following section attempts to elucidate some of the assumptions and simplifica-

tions that went into the simulation framework (Appendix D.1) and algorithm comparisons (Appendix D.2).

D.1 Latency simulation limitations

The Monte Carlo client latency simulations presented in Section 3 provide new tools for analyzing the role of fast and slow clients in simulations. That being said, there are limitations to the MC.

1. The log-normal distribution worked well from a practical standpoint for parameterizing the latency factors. However, the individual latency factor distributions are highly dependent on the devices and characteristics of the clients involved in FL. This work would benefit from explorations of additional functional forms for the latency. Future works might also consider adopting distributions from production applications directly.
2. Communication time was modeled as a single parameter ($T_{\text{Communication}}$) in this work. But it would be more realistic to decompose the communication time into upload and download times that scale with the bytes transferred in each direction. This would enable explorations of the trade-offs between client computation time and communication cost. In particular, this constant parameter affects latency comparisons with **FARe-DUST**, which has a larger download cost as a result of the teacher model. It was determined that this additional latency term would have only a small effect on the overall simulated latency (on the order of a few percent) and would not change the observations presented in this work.
3. The per-example computation cost was the same for all examples on a given client in this work. But for sequential modeling tasks (i.e. `StackOverflow`), the per-example compute time should scale with the number of sequential elements (such as tokens or time frames). This change would help explore scenarios in which straggler clients are defined by the length of data sequences, rather than just the number or type of sequences as in this work.
4. This work assumes that the communication latency and per-example training latency distributions are uncorrelated. However, real-world applications of FL probably have more complex correlations. New devices, for instance, may process training examples more rapidly and typically support faster network connections.
5. The role of client sampling was not explored in this work. In practice, clients in FL are not sampled uniformly at random from the population. In fact, it is quite likely that straggler clients are also less likely to check-in for training, presenting yet another obstacle to learning from them in production settings. Explorations of the relationship between client sampling probability and client latency are possible directions for future work.

D.2 Algorithm comparison limitations

We endeavored to provide fair comparisons of existing FL algorithms (**FedAvg**, **FedAdam**, and **FedBuff**) with our new algorithms (**FRe-DUST** and **FeAST-on-MSG**) on a variety of benchmark tasks. Some limitations of our tuning procedures and comparisons of results are summarized below.

1. Results with time-limited client computations were only reported for one time limit (the 75th percentile client training time for one local epoch). We did not scan the value of the client computation time limit, which would have yielded a range of accuracy-time trade-offs.
2. Upload and download times were excluded from the client computation time limits, meaning that stragglers with high communication latencies were not helped with this technique. While incorporating (post-training) upload times is impossible, it might be possible to estimate future upload times and use those to set time limits on the overall client computation process.
3. All of the algorithms presented have many levers to tune the accuracy-time trade-offs. Examples include the over-selection fraction, the max wait time for **FeAST-on-MSG**, the buffer size and max concurrency for **FedBuff**, and more. We did not present complete scans of these values, which would have elucidated the accuracy-time trade-offs. Instead, we identified individual working points which we believed to be representative of the best trade-offs provided by each algorithm.
4. The **FedBuff** algorithm was tuned for each dataset and latency model. However, we failed to find a configuration for StackOverflow that converged smoothly and rapidly. We believe that increasing the max concurrency beyond the values which we scanned, combined with larger buffer sizes, might lead to faster convergence than in the results that were reported.
5. Similarly, **FeAST-on-MSG** was tuned for each dataset and latency model. In several cases, the model was over-tuned for straggler accuracy. That is, it achieved remarkably high straggler accuracy, but at the cost of significantly lower total accuracy. We believe that better trade-offs between total accuracy and straggler accuracy could be identified with a modified hyper-parameter tuning objective.
6. For hyper-parameter selection, we chose to maximize the straggler accuracy. While this ultimately produced models with higher overall accuracy in many cases, it would be better to identify a more balanced hyper-parameter tuning objective in future works.

E Broader impact

The FL literature has noted (e.g. in Wang et al. [31], Kairouz et al. [2]) that while the FL platform enables the possibility of broader inclusion of data from minority populations, it is generally a non-trivial matter to correct for biases arising from systems and data heterogeneity.

Table 6: Client statistics for the EMNIST, CIFAR-100, and StackOverflow datasets as described in Section 4.

Task	Standard clients	Straggler clients	Total clients
EMNIST	2,600	800	3,400
CIFAR-100	375	125	500
StackOverflow	248,595	93,882	342,477

Kairouz et al. [2] states that “... output from devices with faster processors may be over-represented, with these devices likely newer devices and thus correlated with socioeconomic status”. One of the most prevalent forms of FL is one where the participating client devices are mobile phones, and correlations between mobile phone usage and socioeconomic status have been identified (Frias-Martinez and Virseda [55], Steele et al. [56]).

Against this backdrop, the improvements proposed in this paper to better include straggler clients are not merely motivated by improved learning efficiency, but by the potential benefits of reducing bias in FL model training and evaluation. A beneficial societal impact of the production deployment of this work would be improved inclusion of data from poorer populations (via improved inclusion of their ‘straggling’ older model mobile phones) and less-connected populations (via improved inclusion of their ‘straggling’ slower internet connections).

In general, a tension exists in ML and data science between privacy and fairness (e.g., see Section 7.4 in Wang et al. [31]). However, a nice property of the methods described in this paper is that they address data inclusion via a simple and non-private discriminating metric: a client’s total round run time T_{round} . We only focus on methods which allow for improved contribution from clients with the largest T_{round} in a given cohort. There’s no need to do potentially privacy-impacting actions such as e.g. identifying and clustering clients by their data similarity.

F Simulated client latency distributions

This section provides additional information about the simulated client latency distributions introduced in Section 3 as they were applied to the EMNIST, CIFAR-100, and StackOverflow tasks described in Section 4.1. A summary of the client statistics for each task is also provided in Table 6.

F.1 EMNIST client latency distributions

EMNIST client latency distributions are shown in Figure 9, and summary statistics are provided in Table 7. Recall that for EMNIST, straggler clients were defined as the 800 clients with the most examples from digits 0-4, while standard clients were the remaining 2,600 clients that have examples with digits 0-4 removed. For the **per-example** scenario, straggler clients and standard clients shared the same log-normal parameterizations of the latency factors. As a result, straggler clients had comparable latency distributions to standard clients.

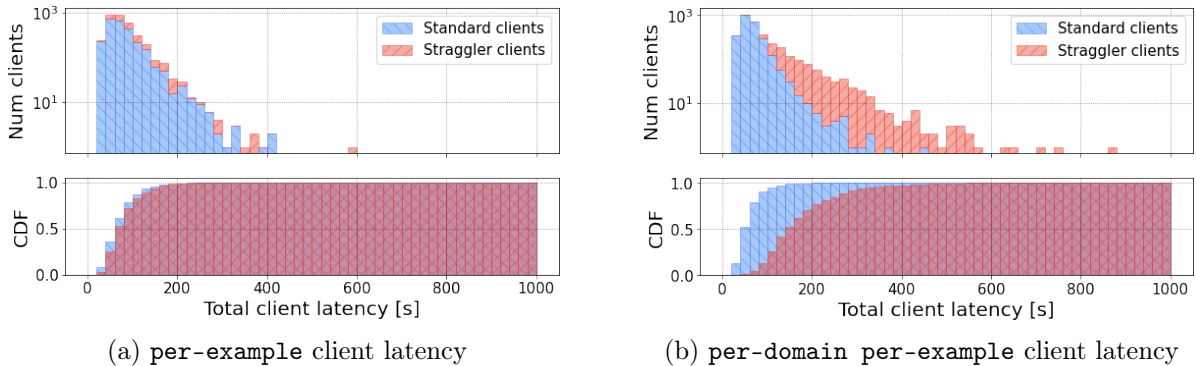


Figure 9: The distribution of total client latencies, in seconds, for the EMNIST dataset. The PDFs (top) are stacked, while the CDFs (bottom) are overlaid. In the **per-example** client latency model (Figure 9a), client latency is a function of the number of training examples per client only, and not data domain. As a result, the standard client distribution and straggler client distribution closely match. In the **per-domain per-example** client latency model (Figure 9b), latency is a function of the number of training examples per client as well as the data domains of the clients. As a result, the straggler client distributions have significantly higher mean values and longer tails than the standard clients.

Table 7: Simulated client latencies with the EMNIST dataset, using the **per-example** client latency model (left) and **per-domain per-example** client latency model (right).

	per-example			per-domain per-example		
	50% [s]	95% [s]	99% [s]	50% [s]	95% [s]	99% [s]
Standard clients	69.89	151.7	223.4	59.35	117.3	194.3
Straggler clients	77.14	160.5	223.8	151.5	323.8	472.0

The median straggler client had slightly more examples than the median standard client (77.14 seconds vs. 69.89 seconds median latency, respectively), due to the fact that examples featuring the digits 0-4 were removed from standard client data partitions. This explains the slightly higher median latency in this scenario. However, both sets of clients had 99th percentile latencies close to 223 seconds.

For the EMNIST **per-domain per-example** client latency scenario, the straggler clients had log-normal parameterizations of the latency factors with larger values of μ and σ . Consequently, the straggler client latencies were typically much longer than those of standard clients. The median straggler client latency was nearly $3\times$ greater than the median standard client latency (151.5 seconds vs 59.35 seconds, respectively).

F.2 CIFAR-100 client latency distributions

CIFAR-100 client latency distributions are shown in Figure 10, and summary statistics are provided in Table 8. Recall that for CIFAR-100, straggler clients were defined as the

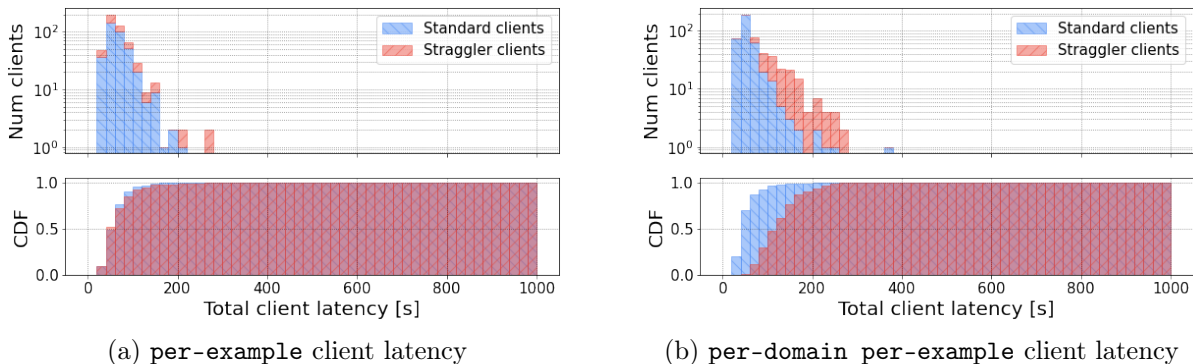


Figure 10: The distribution of total client latencies, in seconds, for the CIFAR-100 dataset. The PDFs (top) are stacked, while the CDFs (bottom) are overlaid. In the **per-example** client latency model (Figure 10a), client latency is a function of the number of training examples per client only, and not data domain. As a result, the standard client distribution and straggler client distribution closely match. In the **per-domain per-example** client latency model (Figure 10b), latency is a function of the number of training examples per client as well as the data domains of the clients. As a result, the straggler client distributions have significantly higher mean values and longer tails than the standard clients.

Table 8: Simulated client latencies with the CIFAR-100 dataset, using the **per-example** client latency model (left) and **per-domain per-example** client latency model (right).

	per-example			per-domain per-example		
	50% [s]	95% [s]	99% [s]	50% [s]	95% [s]	99% [s]
Standard clients	60.21	117.9	193.5	52.04	111.2	154.6
Straggler clients	60.21	117.1	204.7	114.2	259.9	450.6

125 clients with the most examples from the “vehicles 1” and “vehicles 2” coarse classes, while standard clients were the remaining 375 clients that had examples with those classes removed. For the **per-example** scenario, straggler clients and standard clients shared the same log-normal parameterizations of the latency factors. As a result, straggler clients had nearly the same latency distributions as standard clients across all latency percentiles.

For the CIFAR-100 **per-domain per-example** client latency scenario, the straggler clients had log-normal parameterizations of the latency factors with larger values of μ and σ . Consequently, the straggler client latencies were typically much longer than those of standard clients. The median straggler client latency (114.2 seconds) was slower than the 95th percentile standard client latency (111.2 seconds). And stragglers were $3\times$ slower than standard clients at the 99th percentile (450.6 seconds vs. 154.6 seconds, respectively).

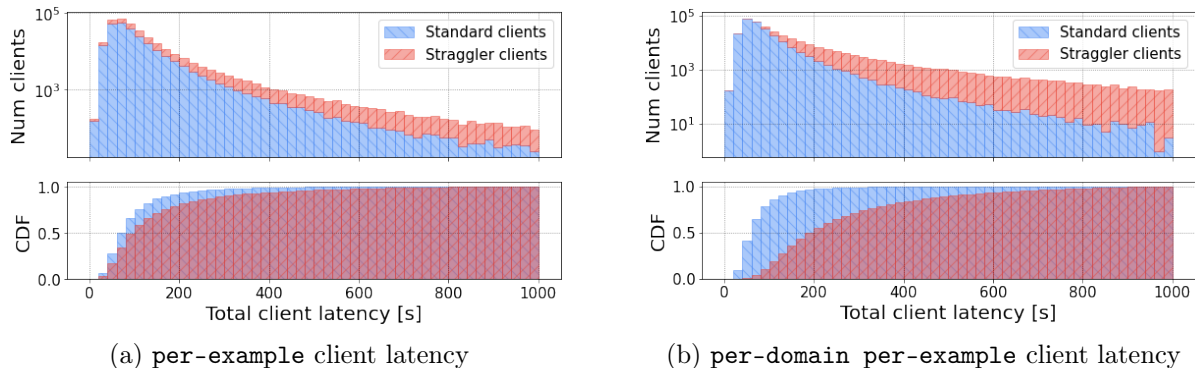


Figure 11: The distribution of total client latencies, in seconds, for the StackOverflow dataset. The PDFs (top) are stacked, while the CDFs (bottom) are overlaid. In the **per-example** client latency model (Figure 11a), client latency is a function of the number of training examples per client only, and not data domain. As a result, the standard domain client distribution and straggler domain client distribution are comparable. The straggler client distribution is a bit longer tailed because clients in the dataset containing questions or answers with the “math” or “c + +” tags had a greater number of associated examples. In the **per-domain per-example** client latency model (Figure 11b), latency is a function of the number of training examples per client as well as the data domains of the clients. As a result, the straggler domain client distributions have significantly higher mean values and longer tails than the standard domain clients.

F.3 StackOverflow client latency distributions

StackOverflow client latency distributions are shown in Figure 11, and summary statistics are provided in Table 9. Recall that for StackOverflow, straggler clients were defined as the 93,882 clients with questions or answers featuring the “math” or “c + +” tags, while the remaining 248,595 standard clients did not feature such examples. For the **per-example** scenario, straggler clients and standard clients shared the same log-normal parameterizations of the latency factors. Even so, straggler clients had longer tailed latency distributions than standard clients. This was due to the fact that authors of “math” and “c + +” posts submitted more questions and answers than the average author, resulting in larger simulated client datasets for stragglers than standard clients. The median straggler client had a total latency of 106.2 seconds, while the median standard client had a latency of 80.39 seconds. But the 99th percentile straggler client latency was 1,811 seconds, significantly greater than the 520.1 seconds for standard clients at the 99th percentile.

For the StackOverflow **per-domain per-example** client latency scenario, the straggler clients had log-normal parameterizations of the latency factors with larger values of μ and σ . Consequently, the straggler client latencies were even longer than those of standard clients. The median straggler client latency (211.2 seconds) was slower than the 95th percentile standard client latency (181.7 seconds). And stragglers were $10\times$ slower than standard clients at the 99th percentile (3,369 seconds vs. 325.9 seconds, respectively).

Table 9: Simulated client latencies with the StackOverflow dataset, using the **per-example** client latency model (left) and **per-domain per-example** client latency model (right).

	per-example			per-domain per-example		
	50% [s]	95% [s]	99% [s]	50% [s]	95% [s]	99% [s]
Standard clients	80.39	255.8	520.1	66.20	181.7	325.9
Straggler clients	106.2	615.5	1,811	211.2	1,167	3,369

Table 10: The default hyper-parameters for FedAvg in this work were based on those quoted in Reddi et al. [3]. Only the cohort size and over-selection cohort size were modified. The parameters below were used for experiments with both the **per-example** and **per-domain per-example** latency scenarios for each task.

Parameter	EMNIST	CIFAR-100	StackOverflow
Client batch size	20	20	16
Client number of epochs	1	1	1
Client learning rate (η_l)	0.1	0.1	0.3
Server learning rate (η_g)	1.0	3.0	1.0
Cohort size (B)	50	20	100
Over-selection cohort size (B_t)	60	24	120

G Algorithm tuning

The FedBuff, FARE-DUST, and FeAST-on-MSG algorithms were tuned individually for each task (EMNIST, CIFAR-100, and StackOverflow) and latency model (**per-example** and **per-domain per-example**). This section describes the hyper-parameter values that were scanned during tuning for each algorithm in order to maximize the straggler accuracy. We also discuss the FedAvg and FedAdam hyper-parameters that were adopted from Reddi et al. [3].

G.1 Synchronous FedAvg and FedAdam baselines

Experiments with FedAvg and FedAdam primarily utilized the optimal hyper-parameters identified in Reddi et al. [3] for the EMNIST, CIFAR-100, and StackOverflow tasks. Two parameters — cohort size and the over-selection cohort size — were modified in order to provide more consistency between experiment trials. Table 10 provides the hyper-parameter values for FedAvg, while Table 11 provides the hyper-parameter values for FedAdam. Note that the same hyper-parameter values were used for each task in experiments with both the **per-example** and **per-domain per-example** client latency scenarios.

Table 11: The default hyper-parameters for FedAdam in this work were also based on those quoted in Reddi et al. [3]. Only the cohort size and over-selection cohort size were adjusted. The parameters below were used for experiments with both the **per-example** and **per-domain per-example** latency scenarios for each task.

Parameter	EMNIST	CIFAR-100	StackOverflow
Client batch size	20	20	16
Client number of epochs	1	1	1
Client learning rate (η_l)	0.03	0.03	0.3
Server learning rate (η_g)	0.003	1.0	0.01
Server Adam β_1	0.9	0.9	0.9
Server Adam β_2	0.99	0.99	0.99
Server Adam ϵ	10^{-4}	10^{-1}	10^{-5}
Cohort size (B)	50	20	100
Over-selection cohort size (B_t)	60	24	120

Table 12: The tuned hyper-parameter values for FedBuff with the **per-example** latency model, along with the operating points that were considered for each parameter. Tuning was performed independently for each task.

Parameter	Values scanned	Tuned value		
		EMNIST	CIFAR-100	StackOverflow
η_l	$\{10^{-4}, 10^{-3}, 10^{-2}, 10^{-1}, 0.3, 1\}$	10^{-1}	10^{-1}	0.3
η_g	$\{10^{-4}, 10^{-3}, 10^{-2}, 10^{-1}, 0.3, 1\}$	1	1	1
B	$\{5, 10, 20, 50\}$	20	20	50
χ	$\{60, 100, 200\}$	100	60	100

G.2 Asynchronous FedBuff baseline tuning

The FedBuff algorithm [11] as described in Section 2 was optimized using two sequential 2D grid searches: first a 2D search of the client learning rate, η_l , and server learning rate, η_g , followed by a search of the number of clients per server update (a.k.a. the buffer size, B), and the maximum client concurrency, χ . The tuned values of the parameters for FedBuff along with the specific operating points considered during tuning are provided in Table 12 for the **per-example** client latency scenario and Table 13 for the **per-domain per-example** client latency scenario.

FedBuff was also explored in conjunction with distillation regularization (with strength parameter ρ), proximal L_2 regularization (with strength parameter ν , and EMA post-processing of weights (with decay strength β). A 1-dimensional scan was performed to tune each parameter once η_g , η_l , B , and χ had already been tuned and fixed. The scanned operating points, as well as the tuned values, are shown in Table 14 for the **per-example** client latency scenario and Tables 15 for the **per-domain per-example** client latency scenario.

Table 13: The tuned hyper-parameter values for FedBuff with the **per-domain per-example** latency model, along with the operating points that were considered for each parameter. Tuning was performed independently for each task.

Parameter	Values scanned	Tuned value		
		EMNIST	CIFAR-100	StackOverflow
η_l	$\{10^{-4}, 10^{-3}, 10^{-2}, 10^{-1}, 1\}$	10^{-2}	10^{-1}	1
η_g	$\{10^{-4}, 10^{-3}, 10^{-2}, 10^{-1}, 1\}$	1	1	10^{-1}
B	$\{5, 10, 20, 50\}$	20	20	50
χ	$\{60, 100, 200\}$	200	60	100

Table 14: The tuned hyper-parameter values for FedBuff with the **per-example** client latency model, along with the operating points that were considered. β is the EMA decay, ρ is the knowledge distillation regularization strength, and ν is the proximal L_2 regularization strength. Tuning was performed independently for each task.

Parameter	Values scanned	Tuned value		
		EMNIST	CIFAR-100	StackOverflow
β	$\{0, 0.9, 0.99, 0.999\}$	0.99	0.9	0.99
ρ	$\{0, 10^{-4}, 10^{-3}, 10^{-2}, 0.1, 0.3, 0.5\}$	0.1	0.1	10^{-2}
ν	$\{0, 10^{-4}, 10^{-3}, 10^{-2}, 0.1, 0.3, 0.5\}$	0.5	0.3	10^{-2}

Table 15: The tuned hyper-parameter values for FedBuff with the **per-domain per-example** client latency model, along with the operating points that were considered. β is the EMA decay, ρ is the knowledge distillation regularization strength, and ν is the proximal L_2 regularization strength. Tuning was performed independently for each task.

Parameter	Values scanned	Tuned value		
		EMNIST	CIFAR-100	StackOverflow
β	$\{0, 0.9, 0.99, 0.999\}$	0.99	0.9	0.99
ρ	$\{0, 10^{-4}, 10^{-3}, 10^{-2}, 0.05, 0.1, 0.3\}$	0.05	0.1	10^{-2}
ν	$\{0, 10^{-4}, 10^{-3}, 10^{-2}, 0.05, 0.1, 0.3\}$	0.05	0.3	10^{-4}

Table 16: The operating points scanned for each FARE-DUST parameter, as well as the optimal values identified for all tasks with the **per-example** latency model. k represents the number of historical teachers, β governs the EMA decay strength, and ρ represents the distillation regularization strength.

Par.	Values scanned	Tuned value		
		EMNIST	CIFAR-100	StackOverflow
k	{1, 2, 5, 10, 20, 50, 200, 500, 2000}	50	50	100
β	{0.0, 0.9, 0.95, 0.99, 0.995, 0.999}	0.99	0.9	0.99
ρ	{0, 10^{-4} , 5×10^{-4} , 10^{-3} , 10^{-2} , 10^{-1} , 1}	0.1	0.1	0.0005

Table 17: The operating points scanned for each FARE-DUST parameter, as well as the optimal values identified for all tasks with the **per-domain per-example** latency model. k represents the number of historical teachers, β governs the EMA decay strength, and ρ represents the distillation regularization strength.

Par.	Values scanned	Tuned value		
		EMNIST	CIFAR-100	StackOverflow
k	{1, 2, 5, 10, 20, 50, 200, 500, 2000}	50	50	100
β	{0, 0.9, 0.95, 0.99, 0.995, 0.999}	0.99	0.9	0.99
ρ	{0, 10^{-4} , 5×10^{-4} , 10^{-3} , 10^{-2} , 10^{-1} , 1}	0.1	0.1	0.0005

G.3 FARE-DUST tuning

Three parameters were tuned for the FARE-DUST algorithm introduced in Section 2.2: the number of historical teachers (k), the EMA decay strength (β), and the distillation regularization strength (ρ). The tuning search was conducted on the outer product of the operating points listed in Table 16. The optimal values are also provided in Table 16 for the **per-example** client latency scenario and Table 17 for the **per-domain per-example** client latency scenario. FARE-DUST was used in conjunction with the FedAdam server optimizer. Default values for FedAdam from Appendix G.1 were used without tuning for all other hyper-parameters.

G.4 FeAST-on-MSG tuning

Three parameters were tuned for the FeAST-on-MSG algorithm introduced in Section 2.3: the server learning rate η_g , the EMA decay strength β , and the auxiliary learning rate η_a . Instead of directly tuning η_a , we formed $\eta_a = \kappa \eta_g$ and tuned $\kappa \in [0, 1]$. Tuning was performed on the outer product of the operating points listed in Table 18. The optimal values identified by this grid search are also provided in Table 18 for the **per-example** client latency model and Table 19 for the **per-domain per-example** client latency model. The maximum wait time was set to an extremely high (but finite) value of $\tau_{\max} = 100,000$ seconds for all experiments.

Table 18: The **FeAST-on-MSG** algorithm parameters, listed with the operating points scanned during tuning and the optimal values for each task with the **per-example** client latency scenario. η_g represents the server learning rate, β is the EMA decay strength, and $\kappa = (\eta_a/\eta_g)$ governs the auxiliary learning rate.

Par.	Values scanned	Tuned value		
		EMNIST	CIFAR-100	StackOverflow
η_g	{0.003, 0.006, 0.01, 0.03, 0.06, 0.1, 0.2}	0.006	0.2	0.01
β	{0.9, 0.95, 0.99, 0.995, 0.999}	0.95	0.995	0.995
κ	{0, 0.2, 0.5, 0.8, 0.9, 1.0}	0	0.5	0

Table 19: The **FeAST-on-MSG** algorithm parameters, listed with the operating points scanned during tuning and the optimal values for each task with the **per-domain per-example** client latency scenario. η_g represents the server learning rate, β is the EMA decay strength, and $\kappa = (\eta_a/\eta_g)$ governs the auxiliary learning rate.

Par.	Values scanned	Tuned value		
		EMNIST	CIFAR-100	StackOverflow
η_g	{0.003, 0.006, 0.01, 0.03, 0.06, 0.1, 0.2}	0.006	0.2	0.006
β	{0.9, 0.95, 0.99, 0.995, 0.999}	0.99	0.995	0.95
κ	{0, 0.2, 0.5, 0.8, 0.9, 1.0}	0.9	0.5	0.2

The **FeAST-on-MSG** algorithm was used in conjunction with the **FedAvg** server optimizer function. Other than the explicitly specified exceptions, the default hyper-parameter values for **FedAvg** from Appendix G.1 were used for experiments with **FeAST-on-MSG**.

H Full results

This section contains the complete results for experiments with the EMNIST, CIFAR-100, and StackOverflow tasks combined with the **per-example** and **per-domain per-example** client latency scenarios. 10 independent trials were performed using identical hyper-parameters but different random initializations of the trainable variables for each algorithm, task, and latency scenario. Summaries of final evaluation metrics quote the median and 90% confidence interval values from these 10 trials.

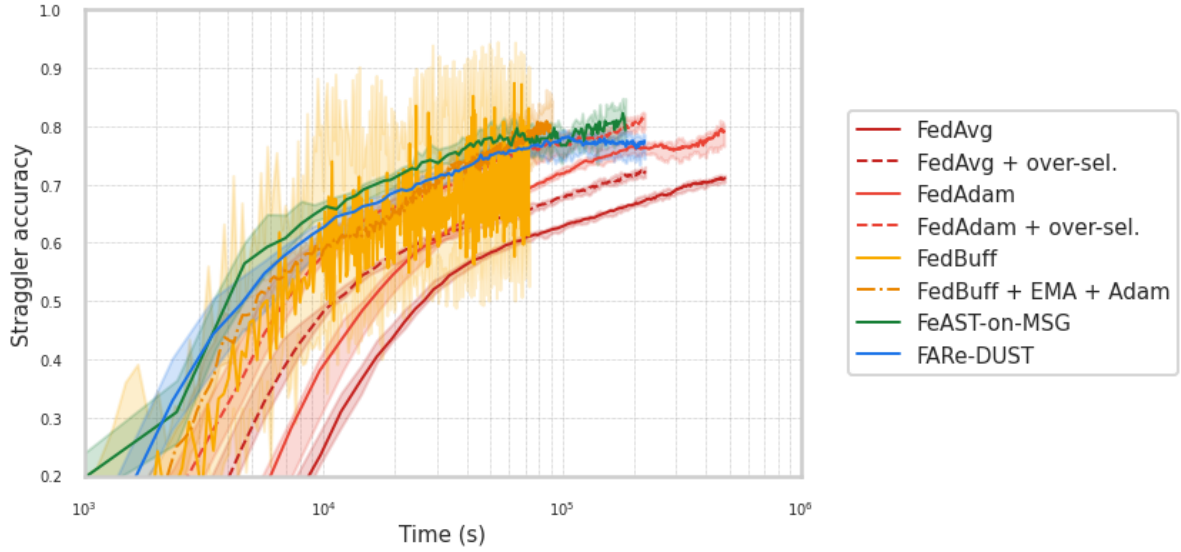
- Results for EMNIST with the **per-example** client latency scenario.
 - Table 20: summary of the final evaluation metrics, with algorithms sorted in descending order of straggler accuracy.
 - Figure 12a: straggler accuracy as a function of wall clock training time.
 - Figure 12b: total accuracy as a function of wall clock training time.

- Figure 13a: the final straggler accuracy as a function of the final total accuracy.
- Figure 13b: the final straggler accuracy as a function of total wall clock training time.
- Results for EMNIST with the **per-domain per-example** client latency scenario.
 - Table 21: summary of the final evaluation metrics, with algorithms sorted in descending order of straggler accuracy.
 - Figure 14a: straggler accuracy as a function of wall clock training time.
 - Figure 14b: total accuracy as a function of wall clock training time.
 - Figure 15a: the final straggler accuracy as a function of the final total accuracy.
 - Figure 15b: the final straggler accuracy as a function of total wall clock training time.
- Results for CIFAR-100 with the **per-example** client latency scenario.
 - Table 22: summary of the final evaluation metrics, with algorithms sorted in descending order of straggler accuracy.
 - Figure 16a: straggler accuracy as a function of wall clock training time.
 - Figure 16b: total accuracy as a function of wall clock training time.
 - Figure 17a: the final straggler accuracy as a function of the final total accuracy.
 - Figure 17b: the final straggler accuracy as a function of total wall clock training time.
- Results for CIFAR-100 with the **per-domain per-example** client latency scenario.
 - Table 23: summary of the final evaluation metrics, with algorithms sorted in descending order of straggler accuracy.
 - Figure 18a: straggler accuracy as a function of wall clock training time.
 - Figure 18b: total accuracy as a function of wall clock training time.
 - Figure 19a: the final straggler accuracy as a function of the final total accuracy.
 - Figure 19b: the final straggler accuracy as a function of total wall clock training time.
- Results for StackOverflow with the **per-example** client latency scenario.
 - Table 24: summary of the final evaluation metrics, with algorithms sorted in descending order of straggler accuracy.
 - Figure 20a: straggler accuracy as a function of wall clock training time.
 - Figure 20b: total accuracy as a function of wall clock training time.
 - Figure 21a: the final straggler accuracy as a function of the final total accuracy.

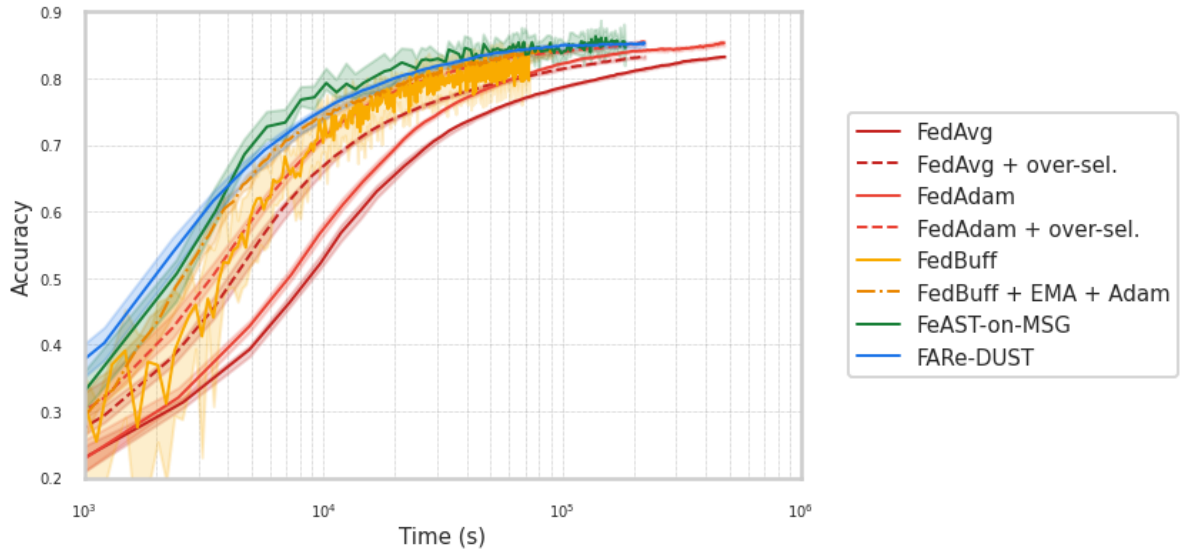
Table 20: The straggler accuracy, total accuracy, and the median total training time for each algorithm with the EMNIST dataset and **per-example** client latency model. Median and 90% CI values from 10 trials are quoted for each metric. Rows are sorted in descending order of straggler accuracy.

Algorithm	Straggler accuracy		Total accuracy		Time [s]
	Median	95% CI	Median	95% CI	
FedAdam + over-sel.	81.3%	[79.6%, 82.2%]	85.4%	[85.2%, 85.7%]	221,268
FeAST-on-MSG	81.0%	[78.5%, 84.8%]	85.2%	[84.4%, 87.7%]	184,630
FedAdam	79.1%	[76.6%, 80.1%]	85.3%	[84.9%, 85.6%]	475,782
FedBuff + EMA + Adam	77.8%	[75.9%, 84.4%]	84.2%	[83.3%, 84.9%]	90,534
FARe-DUST	77.5%	[74.4%, 78.6%]	85.3%	[84.7%, 85.4%]	221,166
FedAvg + over-sel.	72.3%	[71.2%, 73.1%]	83.3%	[83.0%, 83.4%]	222,279
FedAvg + time limit	71.8%	[70.8%, 72.5%]	83.2%	[83.0%, 83.3%]	173,012
FedAvg	71.1%	[70.5%, 71.6%]	83.2%	[83.1%, 83.3%]	479,538
FedBuff + L2 reg.	69.0%	[67.7%, 69.8%]	83.2%	[82.8%, 83.5%]	90,547
FedBuff + EMA	68.9%	[67.2%, 69.6%]	82.8%	[82.3%, 83.0%]	72,554
FedBuff + KD reg.	68.6%	[67.6%, 69.6%]	82.9%	[82.5%, 83.1%]	90,503
FedBuff	61.2%	[52.5%, 79.6%]	79.7%	[77.3%, 84.3%]	72,480

- Figure 21b: the final straggler accuracy as a function of total wall clock training time.
- Results for StackOverflow with the **per-domain per-example** client latency scenario.
 - Table 25: summary of the final evaluation metrics, with algorithms sorted in descending order of straggler accuracy.
 - Figure 22a: straggler accuracy as a function of wall clock training time.
 - Figure 22b: total accuracy as a function of wall clock training time.
 - Figure 23a: the final straggler accuracy as a function of the final total accuracy.
 - Figure 23b: the final straggler accuracy as a function of total wall clock training time.

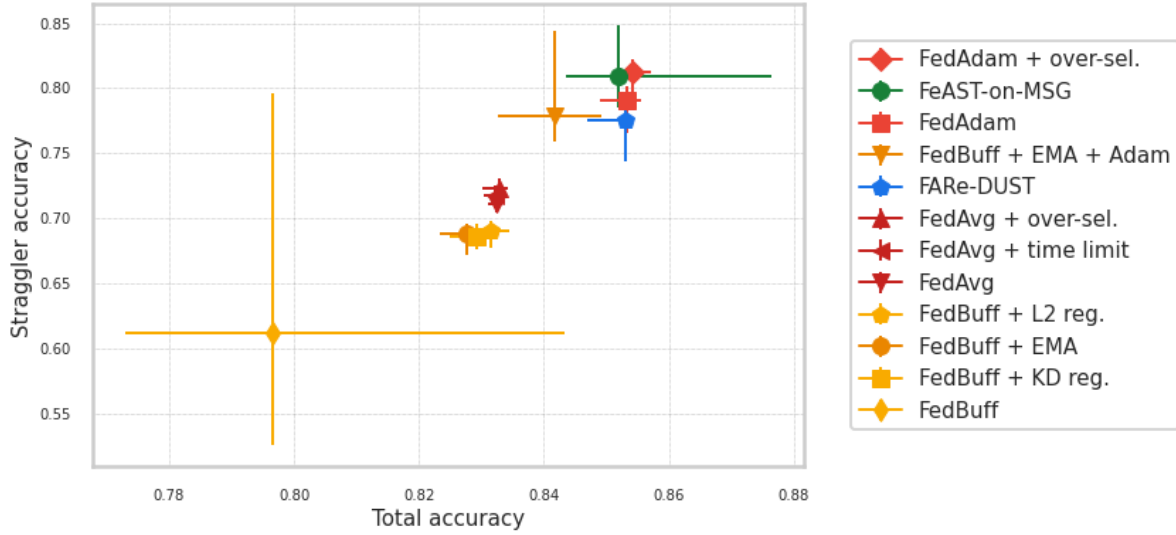


(a) Straggler accuracy as a function of wall clock training time.

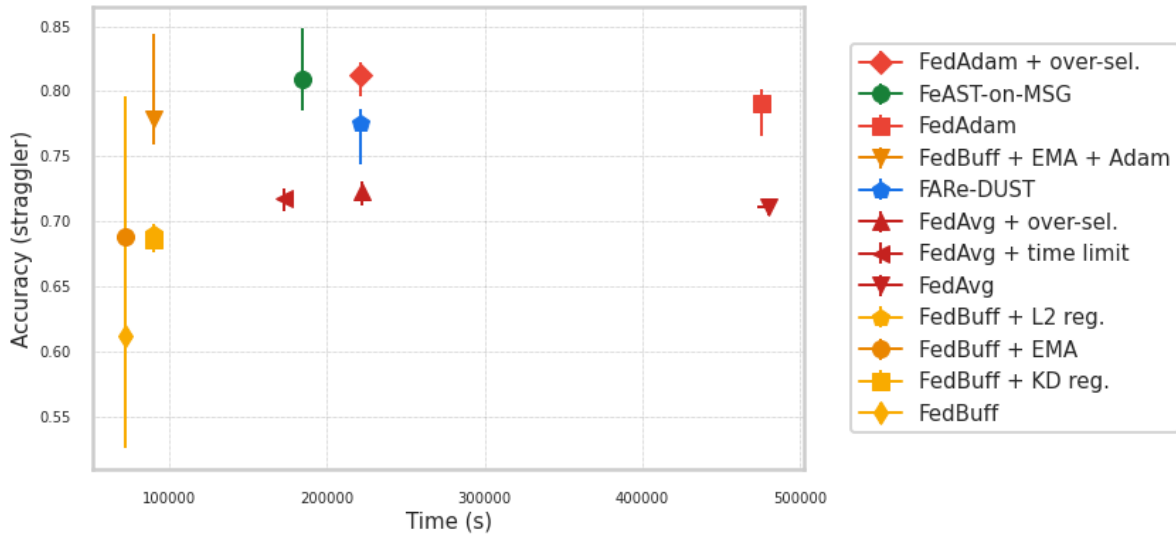


(b) Total accuracy as a function of wall clock training time.

Figure 12: Straggler accuracy (12a) and total accuracy (12b) as a function of wall clock training time for EMNIST with the `per-example` client latency scenario. Median and 90% confidence interval values from 10 trials are illustrated with lines and bands, respectively.



(a) Straggler accuracy as a function of total accuracy.



(b) Straggler accuracy as a function of total training time.

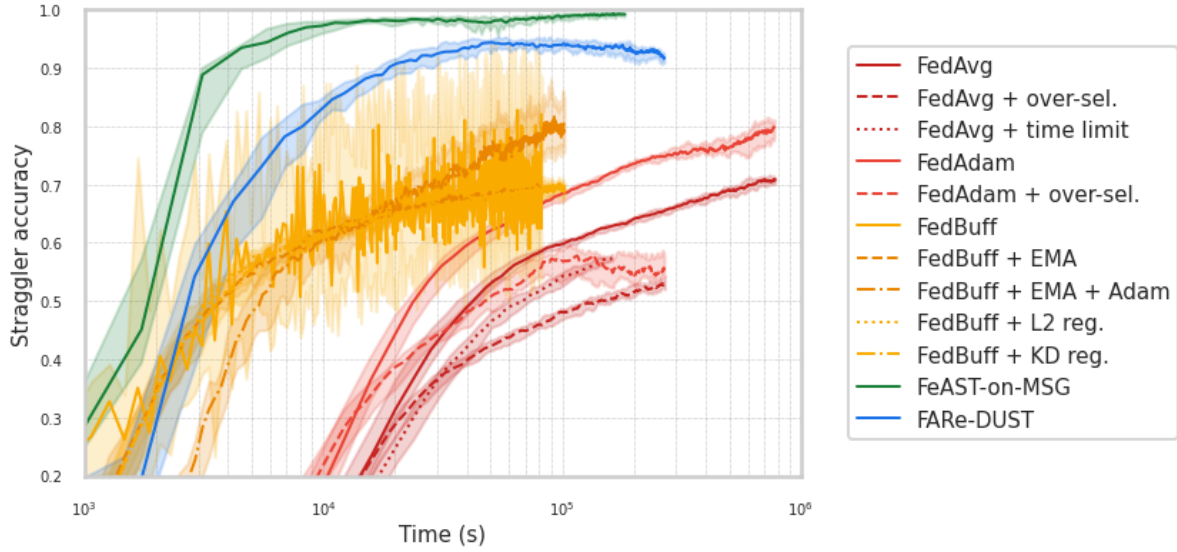
Figure 13: Final straggler accuracy as a function of total accuracy (13a) and as a function of total wall clock training time (13b) for EMNIST with the per-example client latency scenario. Median and 90% confidence interval values from 10 trials are illustrated with points and error bars, respectively.

Table 21: The straggler accuracy, total accuracy, and the total training time for each algorithm with the EMNIST dataset and per-domain per-example client latency model. Median and 90% CI values from 10 trials are quoted for each metric. Rows are sorted in descending order of straggler accuracy.

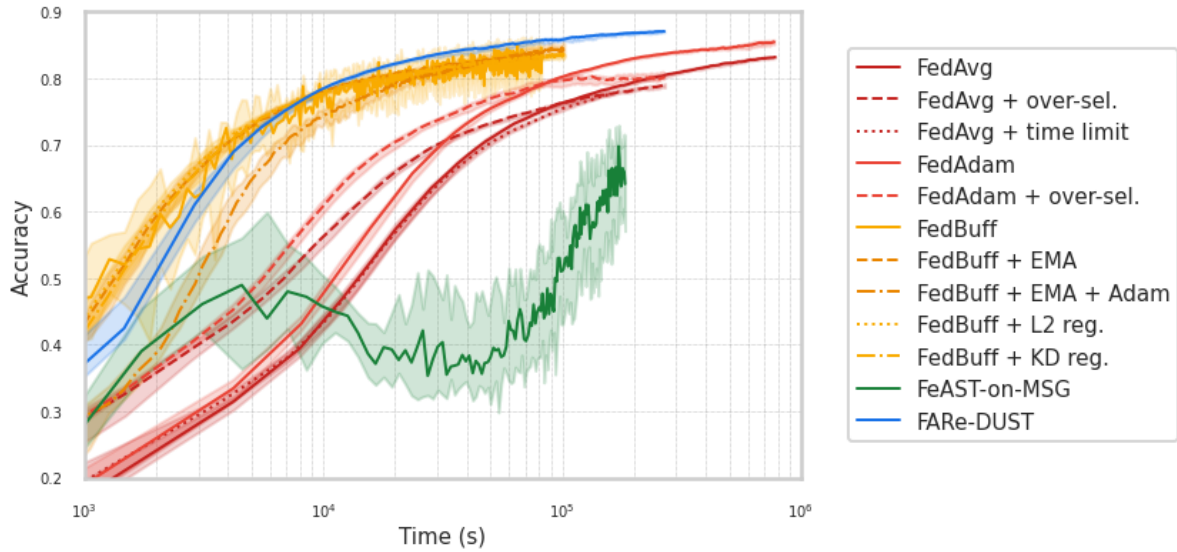
Algorithm	Straggler accuracy		Total accuracy		Time [s]
	Median	95% CI	Median	95% CI	
FeAST-on-MSG	99.2%	[98.9%, 99.4%]	65.2%	[61.8%, 70.6%]	184,565
FARe-DUST	91.7%	[91.0%, 92.5%]	87.0%	[86.9%, 87.2%]	267,541
FedBuff	82.0%	[65.2%, 88.5%]	84.6%	[81.6%, 85.8%]	81,798
FedAdam	79.8%	[77.8%, 81.1%]	85.4%	[85.1%, 85.7%]	771,556
FedBuff + EMA + Adam	79.4%	[76.5%, 84.5%]	84.3%	[84.1%, 85.1%]	102,138
FedAvg	70.8%	[70.3%, 71.2%]	83.2%	[83.0%, 83.2%]	779,631
FedBuff + EMA	69.5%	[68.4%, 70.2%]	83.4%	[83.1%, 83.6%]	81,902
FedBuff + KD reg.	69.1%	[68.3%, 69.8%]	83.4%	[83.2%, 83.6%]	102,150
FedBuff + L2 reg.	68.9%	[68.1%, 70.0%]	83.4%	[83.1%, 83.6%]	102,115
FedAvg + time limit	57.8%	[57.3%, 58.2%]	77.9%	[77.8%, 78.0%]	171,958
FedAdam + over-sel.	55.8%	[54.2%, 57.8%]	80.2%	[79.9%, 80.8%]	267,422
FedAvg + over-sel.	53.2%	[52.0%, 54.2%]	79.0%	[78.6%, 79.2%]	269,295

Table 22: The straggler accuracy, total accuracy, and the total training time for each algorithm with the CIFAR-100 dataset and per-example client latency model. Median and 90% CI values from 10 trials are quoted for each metric. Rows are sorted in descending order of straggler accuracy.

Algorithm	Straggler accuracy		Total accuracy		Time [s]
	Median	95% CI	Median	95% CI	
FedAdam + over-sel.	54.0%	[50.7%, 54.9%]	44.1%	[43.0%, 45.5%]	343,556
FARe-DUST	54.0%	[50.1%, 55.7%]	45.6%	[45.5%, 45.8%]	343,502
FeAST-on-MSG	52.5%	[52.3%, 55.2%]	44.2%	[41.5%, 45.1%]	286,516
FedAdam	51.9%	[48.7%, 53.7%]	43.8%	[41.7%, 45.2%]	638,146
FedAvg + over-sel.	49.0%	[47.3%, 52.4%]	42.2%	[41.5%, 43.1%]	343,386
FedBuff + KD reg.	48.3%	[46.7%, 50.2%]	40.7%	[40.4%, 41.2%]	107,530
FedBuff + EMA	47.7%	[46.1%, 49.1%]	40.8%	[39.9%, 41.1%]	107,582
FedBuff + L2 reg.	47.6%	[44.7%, 49.0%]	40.6%	[40.0%, 40.8%]	107,456
FedAvg	46.9%	[44.4%, 48.1%]	40.4%	[39.6%, 40.8%]	638,038
FedBuff	45.3%	[40.8%, 50.4%]	38.3%	[37.6%, 38.9%]	107,582
FedAvg + time limit	44.3%	[42.6%, 46.3%]	38.5%	[38.2%, 38.9%]	263,174

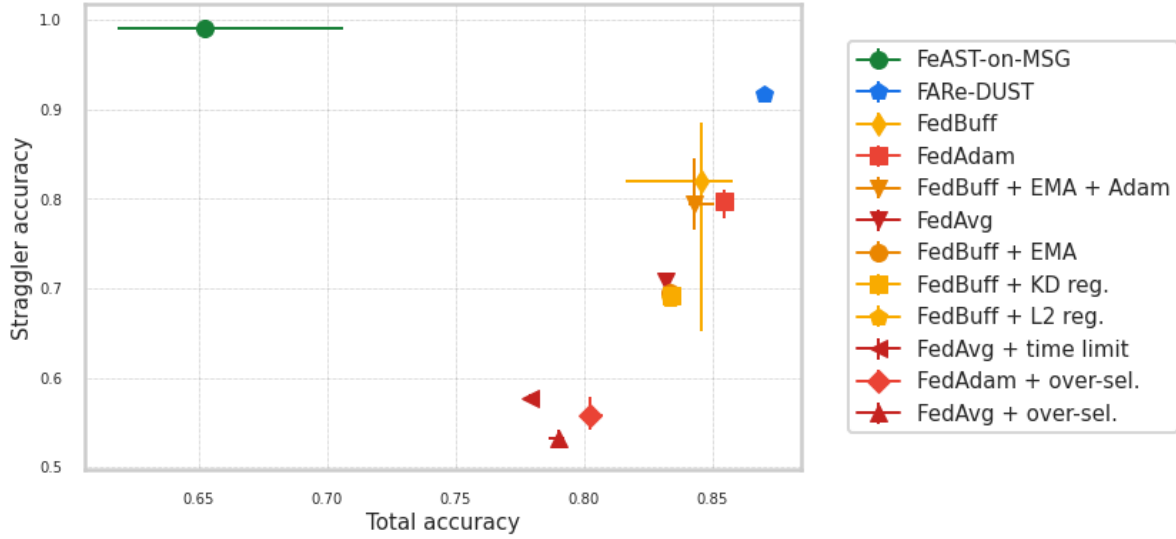


(a) Straggler accuracy as a function of wall clock training time.

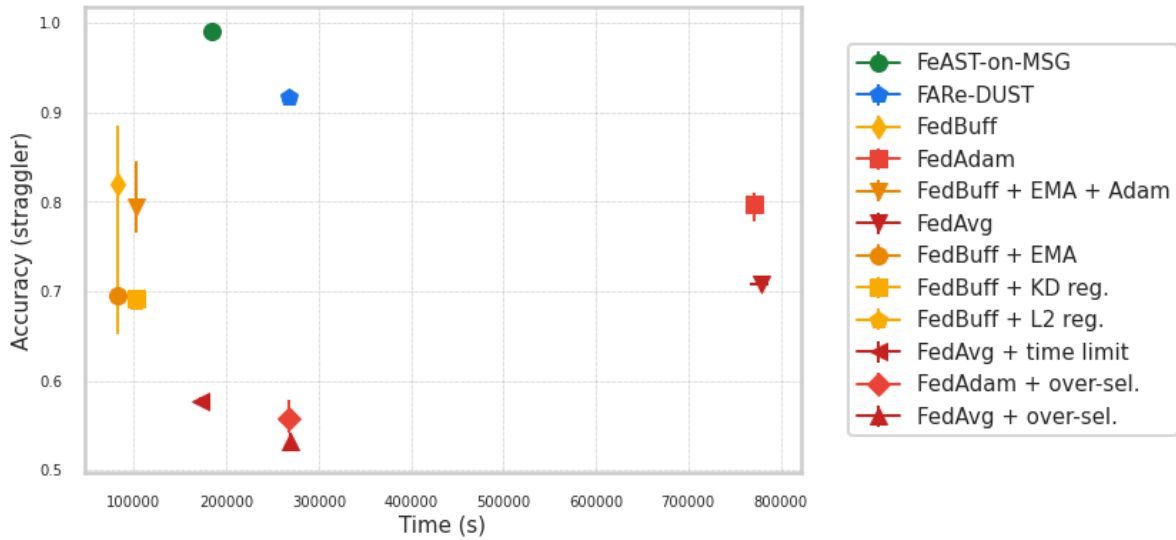


(b) Total accuracy as a function of wall clock training time.

Figure 14: Straggler accuracy (14a) and total accuracy (14b) as a function of wall clock training time for EMNIST with the per-domain per-example client latency scenario. Median and 90% confidence interval values from 10 trials are illustrated with lines and bands, respectively.

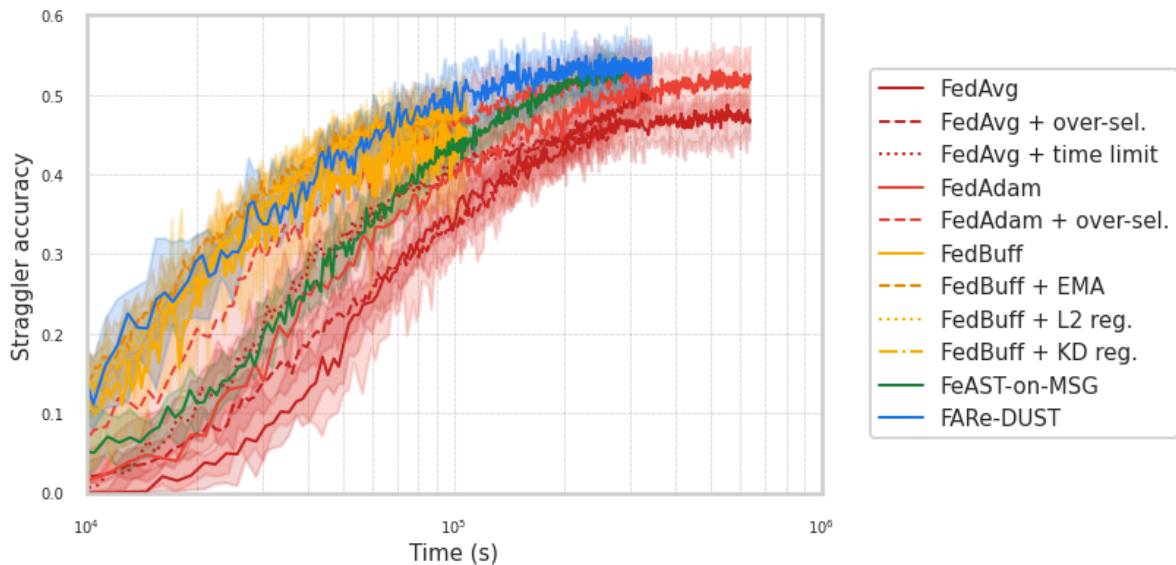


(a) Straggler accuracy as a function of total accuracy.

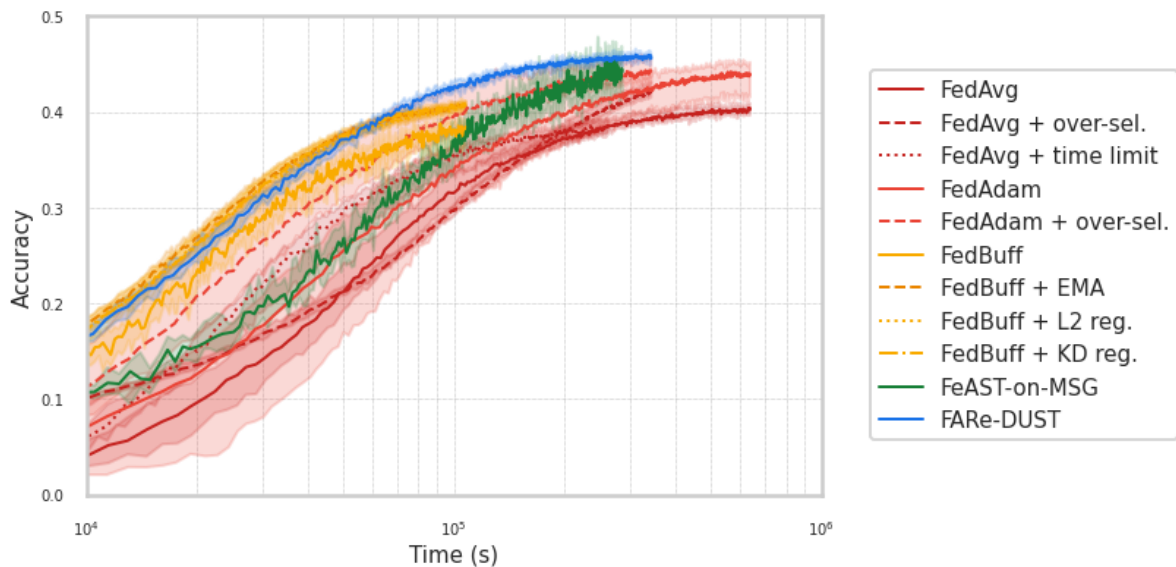


(b) Straggler accuracy as a function of total training time.

Figure 15: Final straggler accuracy as a function of total accuracy (15a) and as a function of total wall clock training time (15b) for EMNIST with the per-domain per-example client latency scenario. Median and 90% confidence interval values from 10 trials are illustrated with points and error bars, respectively.

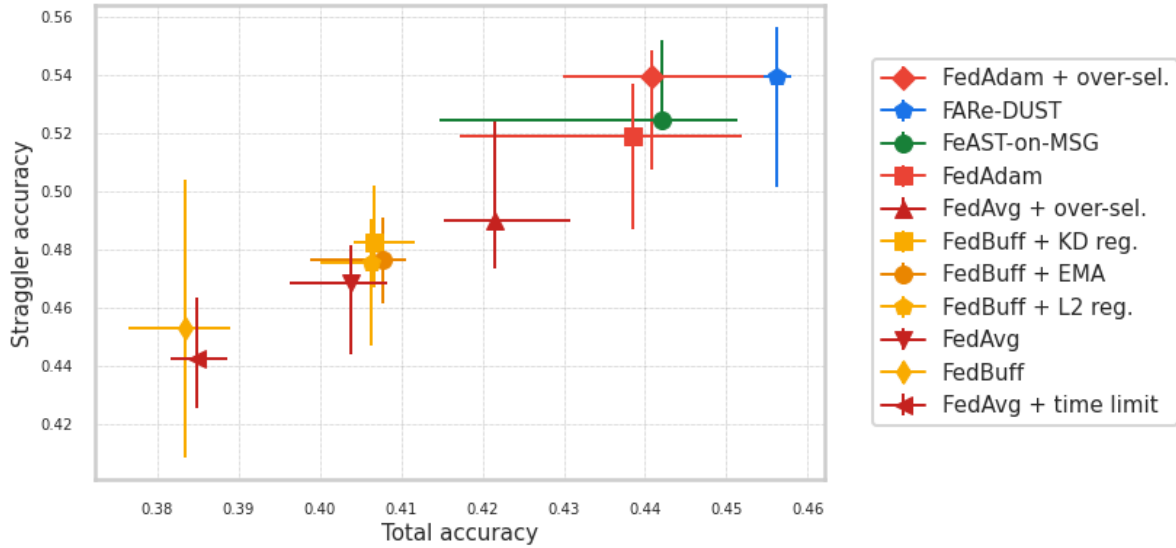


(a) Straggler accuracy as a function of wall clock training time.

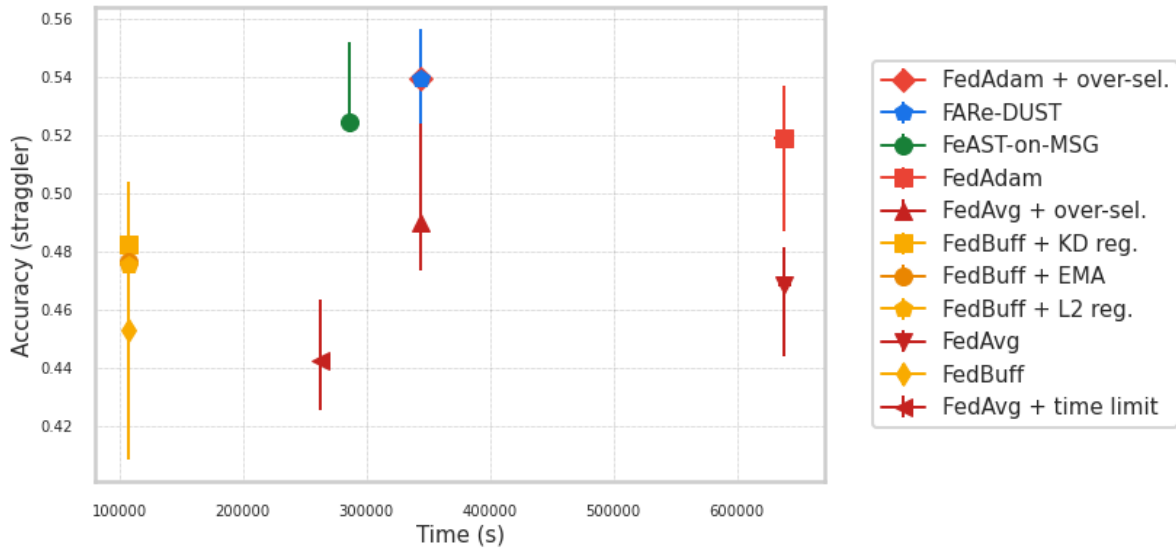


(b) Total accuracy as a function of wall clock training time.

Figure 16: Straggler accuracy (16a) and total accuracy (16b) as a function of wall clock training time for CIFAR-100 with the `per-example` client latency scenario. Median and 90% confidence interval values from 10 trials are illustrated with lines and bands, respectively.



(a) Straggler accuracy as a function of total accuracy.



(b) Straggler accuracy as a function of total training time.

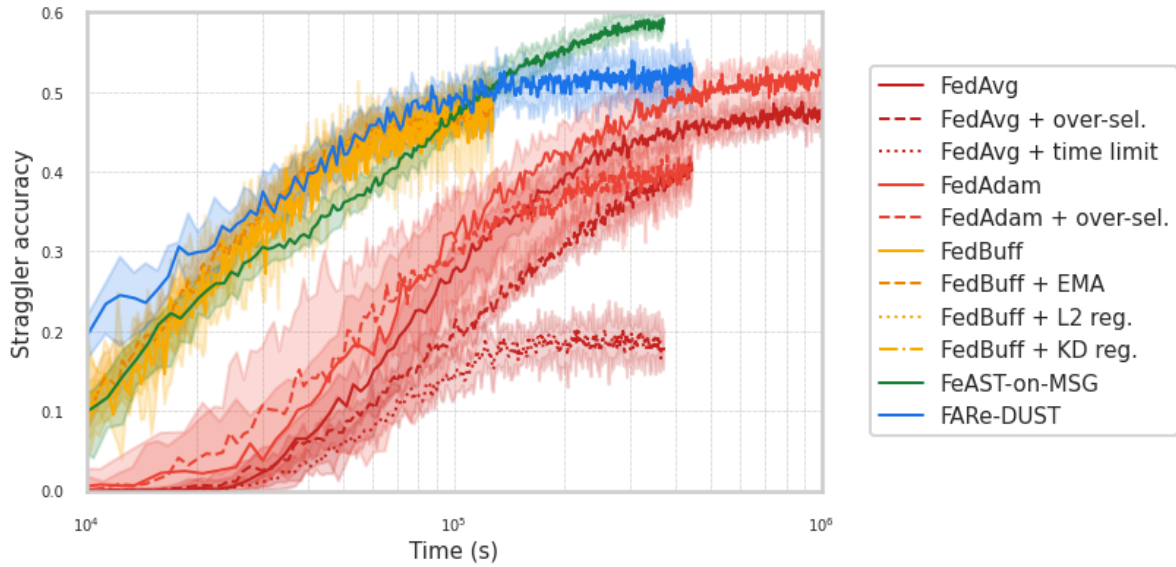
Figure 17: Final straggler accuracy as a function of total accuracy (17a) and as a function of total wall clock training time (17b) for CIFAR-100 with the per-example client latency scenario. Median and 90% confidence interval values from 10 trials are illustrated with points and error bars, respectively.

Table 23: The straggler accuracy, total accuracy, and the total training time for each algorithm with the CIFAR-100 dataset and **per-domain per-example** client latency model. Median and 90% CI values from 10 trials are quoted for each metric. Rows are sorted in descending order of straggler accuracy.

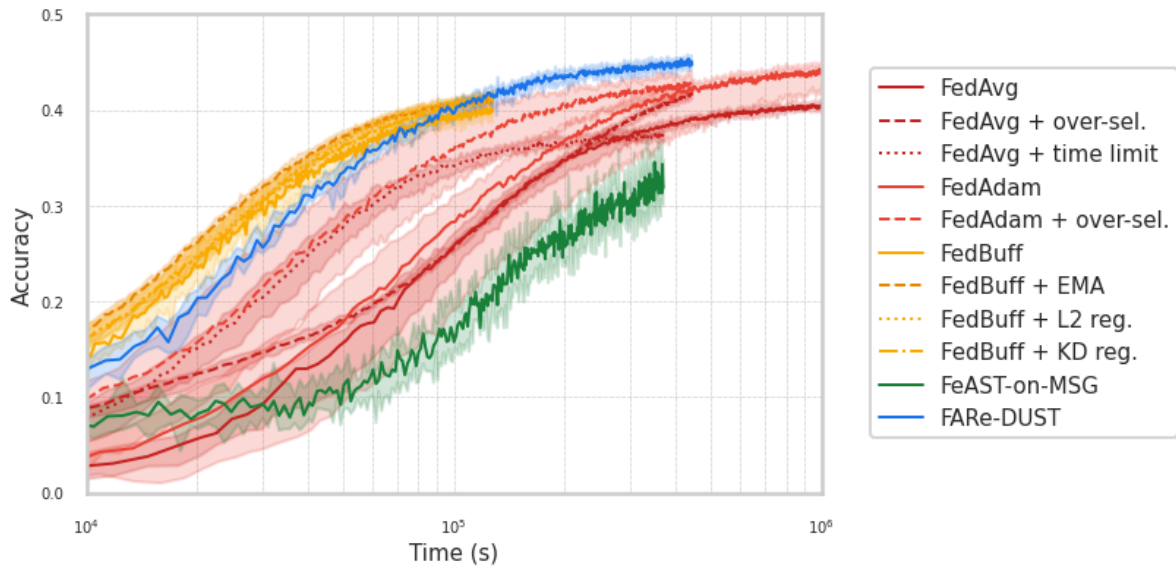
Algorithm	Straggler accuracy		Total accuracy		Time [s]
	Median	95% CI	Median	95% CI	
FeAST-on-MSG	58.6%	[57.6%, 60.4%]	31.9%	[30.1%, 34.8%]	370,547
FedAdam	52.2%	[49.7%, 53.6%]	44.2%	[41.8%, 44.5%]	1,006,330
FARe-DUST	51.9%	[50.1%, 53.7%]	44.7%	[44.5%, 45.2%]	443,452
FedBuff + L2 reg.	48.8%	[47.3%, 50.4%]	41.2%	[41.0%, 42.0%]	127,336
FedBuff + KD reg.	48.6%	[45.9%, 50.5%]	41.1%	[40.7%, 41.5%]	127,375
FedBuff + EMA	48.2%	[46.7%, 49.6%]	41.1%	[40.7%, 41.9%]	127,448
FedAvg	47.9%	[46.1%, 50.1%]	40.4%	[40.0%, 40.9%]	1,004,752
FedBuff	46.4%	[44.9%, 48.4%]	40.0%	[39.1%, 40.3%]	127,208
FedAdam + over-sel.	41.7%	[38.3%, 42.3%]	42.9%	[41.9%, 43.9%]	442,894
FedAvg + over-sel.	40.5%	[39.2%, 42.3%]	41.6%	[41.2%, 41.9%]	443,618
FedAvg + time limit	18.3%	[16.1%, 20.2%]	37.3%	[37.0%, 37.7%]	372,209

Table 24: The straggler accuracy, total accuracy, and the total training time for each algorithm with the StackOverflow dataset and **per-example** client latency model. Median and 90% CI values from 10 trials are quoted for each metric. Rows are sorted in descending order of straggler accuracy.

Algorithm	Straggler accuracy		Total accuracy		Time [s]
	Median	95% CI	Median	95% CI	
FedAdam	25.6%	[25.5%, 25.7%]	25.4%	[25.1%, 25.9%]	3,612,004
FeAST-on-MSG	25.2%	[24.6%, 25.3%]	26.1%	[25.2%, 26.7%]	292,006
FARe-DUST	25.0%	[24.5%, 25.2%]	25.4%	[24.3%, 26.4%]	335,744
FedAdam + over-sel.	24.9%	[23.3%, 25.0%]	25.2%	[21.8%, 25.9%]	336,140
FedBuff + EMA	24.3%	[24.2%, 24.3%]	24.6%	[23.3%, 26.0%]	349,178
FedBuff + KD reg.	24.2%	[24.2%, 24.3%]	23.9%	[23.4%, 25.1%]	350,286
FedAvg	23.7%	[23.5%, 23.8%]	23.6%	[22.2%, 24.6%]	3,584,260
FedBuff	23.3%	[22.3%, 23.6%]	23.4%	[22.3%, 23.7%]	349,257
FedAvg + time limit	21.7%	[21.7%, 21.7%]	22.7%	[21.3%, 23.4%]	287,952
FedAvg + over-sel.	20.9%	[20.8%, 20.9%]	22.4%	[21.1%, 23.2%]	407,588

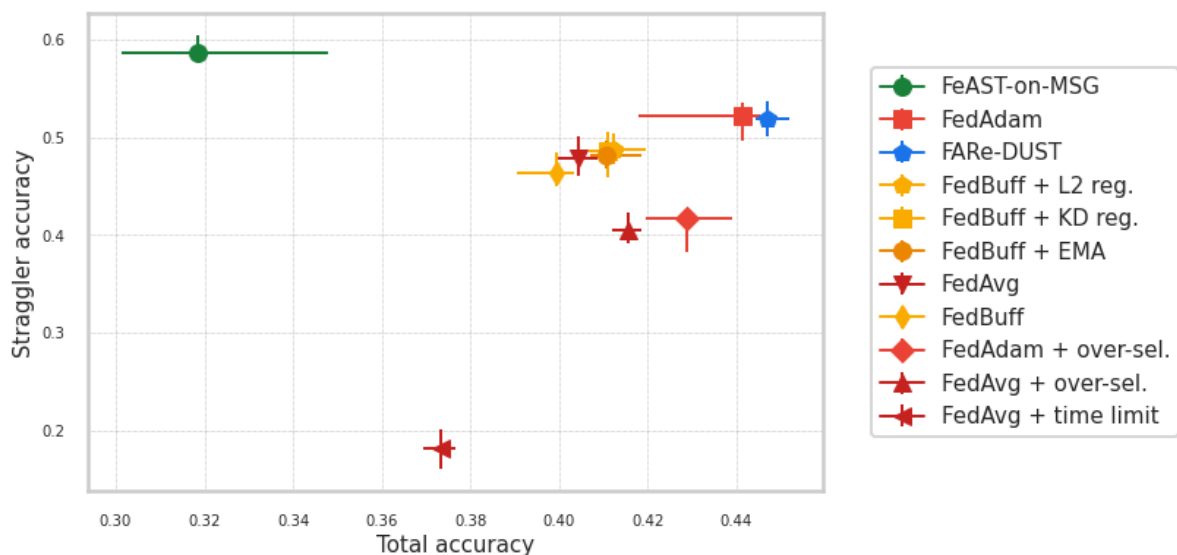


(a) Straggler accuracy as a function of wall clock training time.

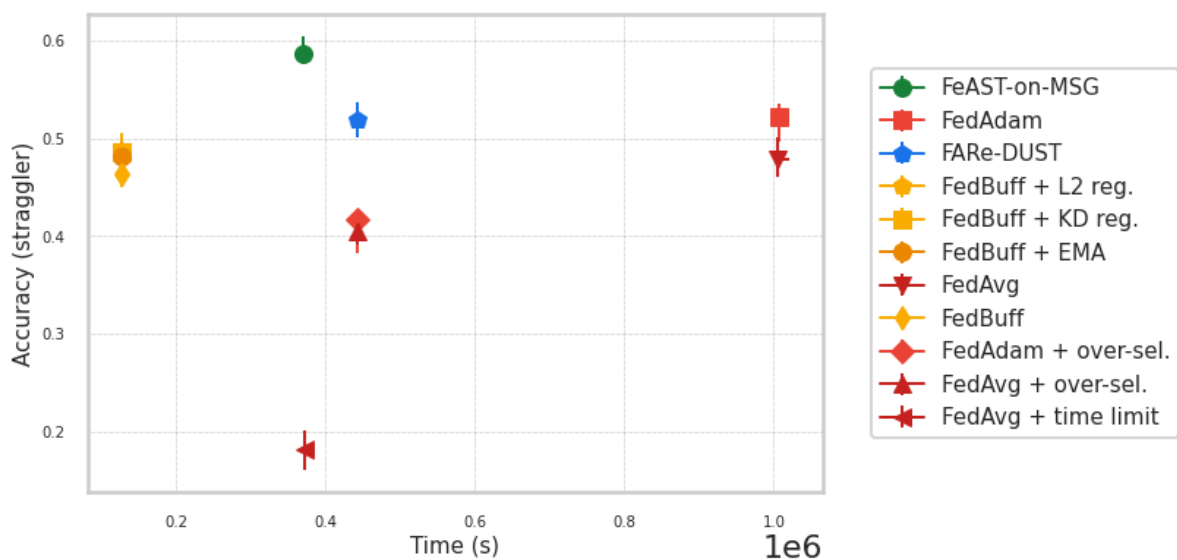


(b) Total accuracy as a function of wall clock training time.

Figure 18: Straggler accuracy (18a) and total accuracy (18b) as a function of wall clock training time for CIFAR-100 with the `per-domain per-example` client latency scenario. Median and 90% confidence interval values from 10 trials are illustrated with lines and bands, respectively.

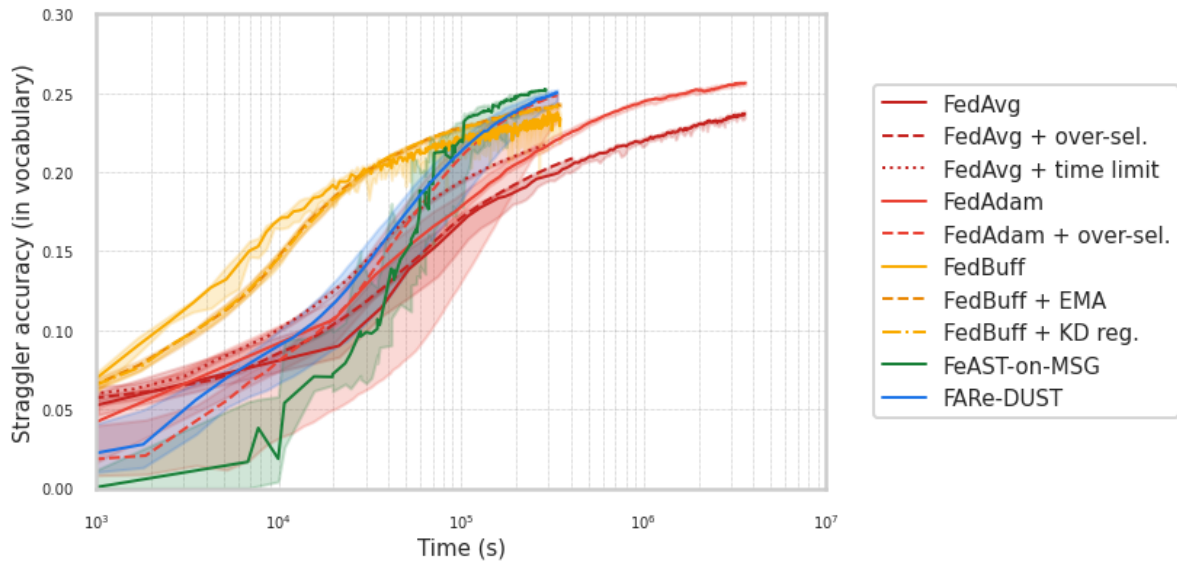


(a) Straggler accuracy as a function of total accuracy.

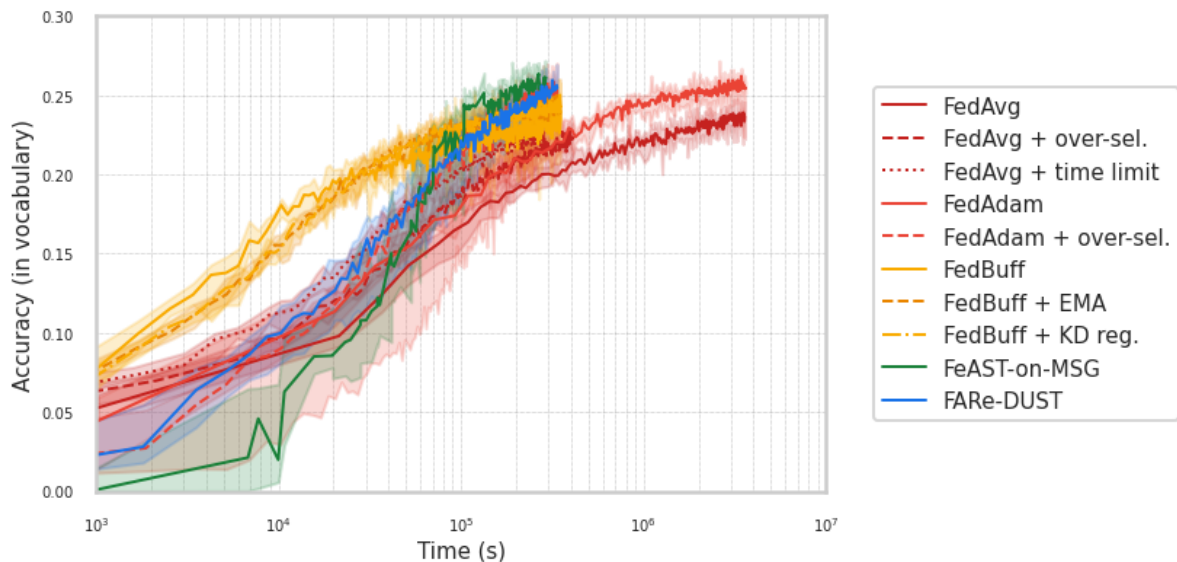


(b) Straggler accuracy as a function of total training time.

Figure 19: Final straggler accuracy as a function of total accuracy (19a) and as a function of total wall clock training time (19b) for CIFAR-100 with the per-domain per-example client latency scenario. Median and 90% confidence interval values from 10 trials are illustrated with points and error bars, respectively.

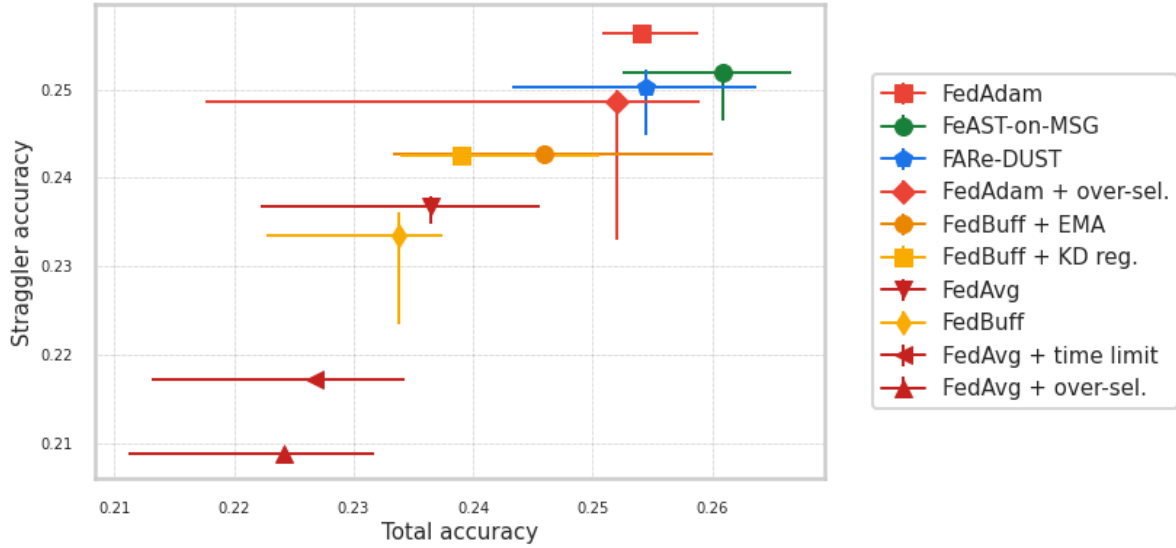


(a) Straggler accuracy as a function of wall clock training time.

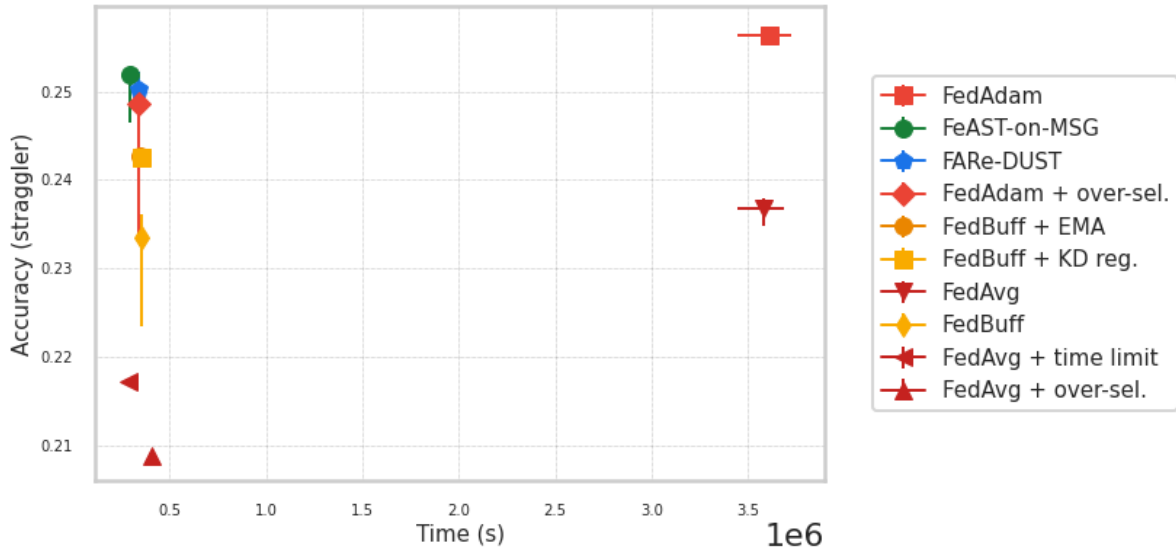


(b) Total accuracy as a function of wall clock training time.

Figure 20: Straggler accuracy (20a) and total accuracy (20b) as a function of wall clock training time for StackOverflow with the **per-example** client latency scenario. Median and 90% confidence interval values from 10 trials are illustrated with lines and bands, respectively.

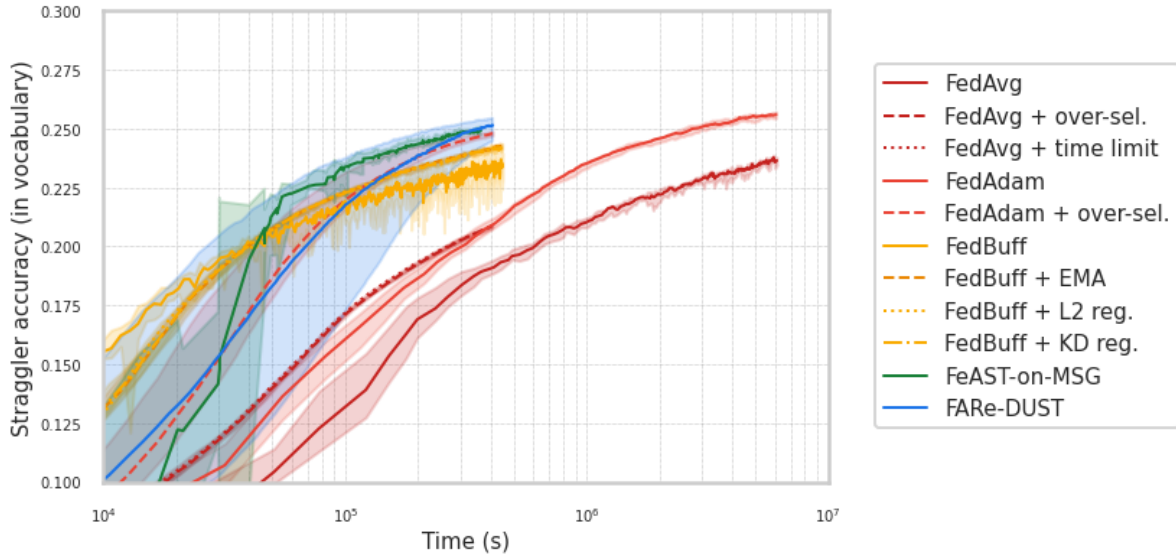


(a) Straggler accuracy as a function of total accuracy.

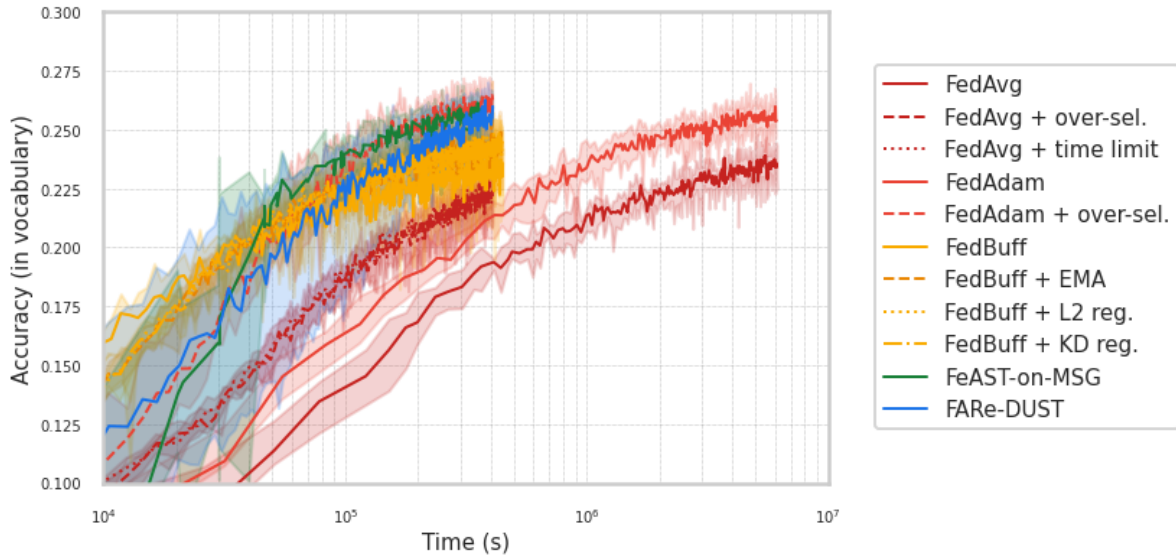


(b) Straggler accuracy as a function of total training time.

Figure 21: Final straggler accuracy as a function of total accuracy (21a) and as a function of total wall clock training time (21b) for StackOverflow with the per-example client latency scenario. Median and 90% confidence interval values from 10 trials are illustrated with points and error bars, respectively.

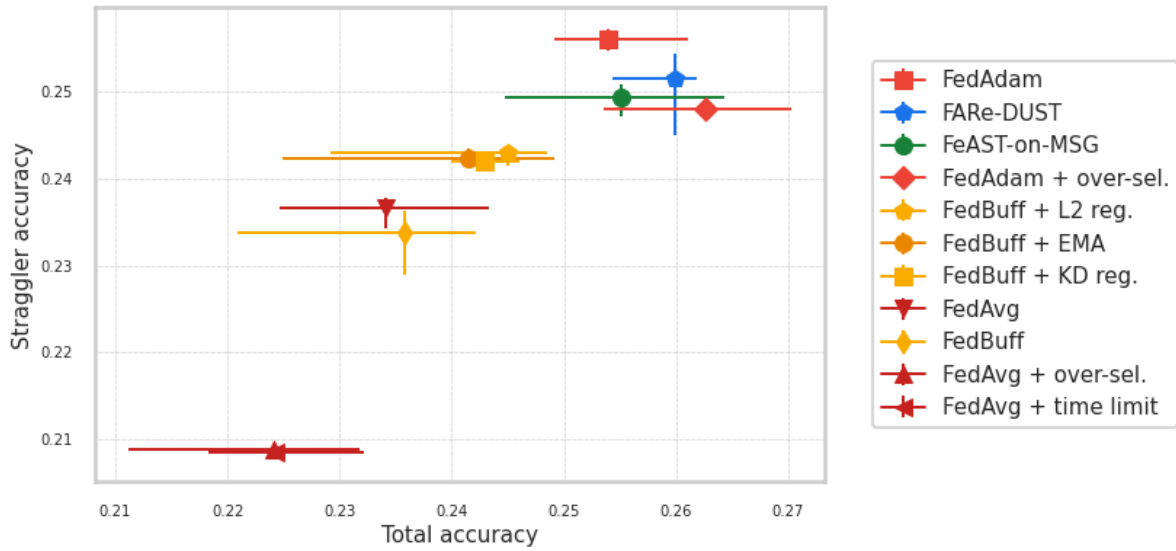


(a) Straggler accuracy as a function of wall clock training time.

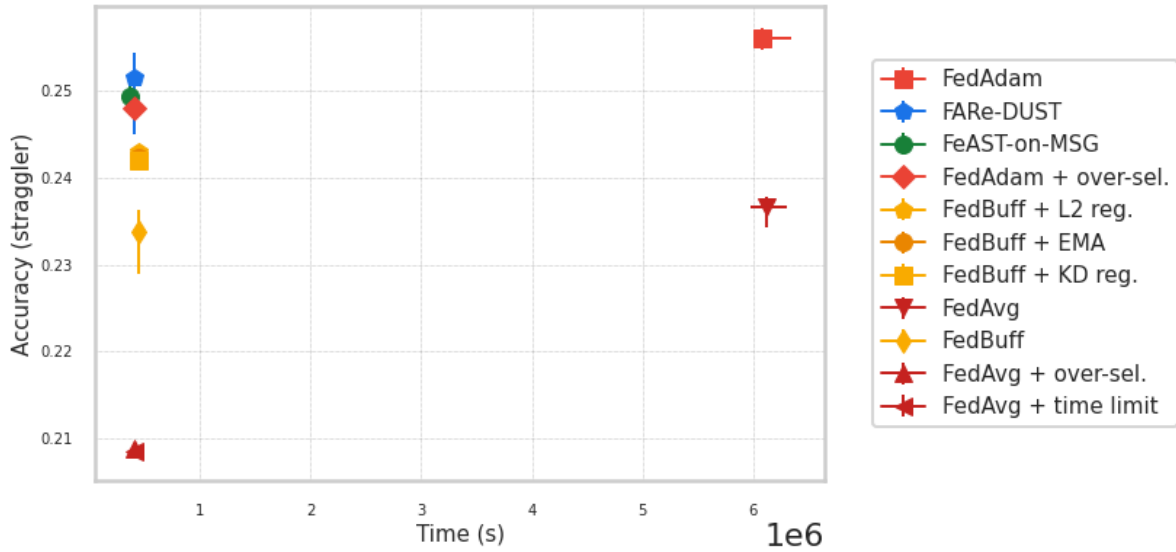


(b) Total accuracy as a function of wall clock training time.

Figure 22: Straggler accuracy (22a) and total accuracy (22b) as a function of wall clock training time for StackOverflow with the **per-domain per-example** client latency scenario. Median and 90% confidence interval values from 10 trials are illustrated with lines and bands, respectively.



(a) Straggler accuracy as a function of total accuracy.



(b) Straggler accuracy as a function of total training time.

Figure 23: Final straggler accuracy as a function of total accuracy (23a) and as a function of total wall clock training time (23b) for StackOverflow with the per-domain per-example client latency scenario. Median and 90% confidence interval values from 10 trials are illustrated with points and error bars, respectively.

Table 25: The straggler accuracy, total accuracy, and the total training time for each algorithm with the StackOverflow dataset and per-domain per-example client latency model. Median and 90% CI values from 10 trials are quoted for each metric. Rows are sorted in descending order of straggler accuracy.

Algorithm	Straggler accuracy		Total accuracy		Time [s]
	Median	95% CI	Median	95% CI	
FedAdam	25.6%	[25.5%, 25.7%]	25.4%	[24.9%, 26.1%]	6,086,590
FARe-DUST	25.1%	[24.5%, 25.4%]	26.0%	[25.4%, 26.2%]	408,276
FeAST-on-MSG	24.9%	[24.7%, 25.1%]	25.5%	[24.5%, 26.4%]	364,537
FedAdam + over-sel.	24.8%	[24.7%, 24.9%]	26.3%	[25.4%, 27.0%]	408,178
FedBuff + L2 reg.	24.3%	[24.1%, 24.4%]	24.5%	[22.9%, 24.9%]	447,008
FedBuff + EMA	24.2%	[24.2%, 24.3%]	24.1%	[22.5%, 24.9%]	443,355
FedBuff + KD reg.	24.2%	[24.1%, 24.2%]	24.3%	[24.0%, 24.6%]	445,861
FedAvg	23.7%	[23.4%, 23.8%]	23.4%	[22.5%, 24.3%]	6,119,154
FedBuff	23.4%	[22.9%, 23.6%]	23.6%	[22.1%, 24.2%]	449,020
FedAvg + over-sel.	20.9%	[20.8%, 20.9%]	22.4%	[21.1%, 23.2%]	407,588
FedAvg + time limit	20.9%	[20.8%, 20.9%]	22.4%	[21.8%, 23.2%]	405,116